PHOTON IMPACT

high-energy plasma physics with $C0_2$ lasers

by David W. Forslund and Philip D. Goldstone

Research on controlled fusion attempts to mimic in the laboratory the thermonuclear burn of stars. At Los Alamos, Antares, a giant $C0_2$ laser, has been dedicated to the hope that eventually small amounts of matter can be imploded to densities and pressures exceeding those in the center of a star by using the power of high-intensity light. Because the physics of laser fusion involves an enormous range of uncharted phenomena, our experiments and theoretical simulations have produced many surprises. For example, in some experiments highly collimated ion jets are seen streaking from the laser target, reminiscent of the huge jets that sometimes streak for millions of parsecs from the centers of distant galaxies. Perhaps we have inadvertently imitated exotic features of the heavens other than thermonuclear burn.

We have also learned that laser fusion will not likely be achieved with CO_2 lasers. Antares and its lower-energy predecessor, Helios, were built to take advantage of the reliability, high repetition rate, and high efficiency of the $C0_2$ laser—features that will be needed for large-scale energy production. With the 10-micrometer (μm) light from these lasers, we have been able to explore pertinent physics carefully, learning, for example, how that physics depends on the intensity and wavelength of the light. Among other things, these experiments have demonstrated emphatically that if laser fusion is to be achieved, wavelengths much shorter than 10 μm are needed. Currently, the laser fusion program at Los Alamos is exploring possibilities for new types of lasers, including the KrF laser, a promising, highly efficient gas laser with 0.25-μm light (see "KrF Laser").

The theoretical effort at Los Alamos that parallels the experimental one has uncovered many of the mechanisms that drive the unusual physics. This interplay between experiment and computer simulation has moved our understanding far beyond the crude knowledge available when laser fusion was first proposed about two decades ago, and many of our original simple models have been altered considerably. Our studies have also greatly enhanced our understanding of plasmas with extremely high energy densities, such as probably exist (albeit on much greater time and space scales) in the atmospheres of white dwarfs or in the cores of galaxies.

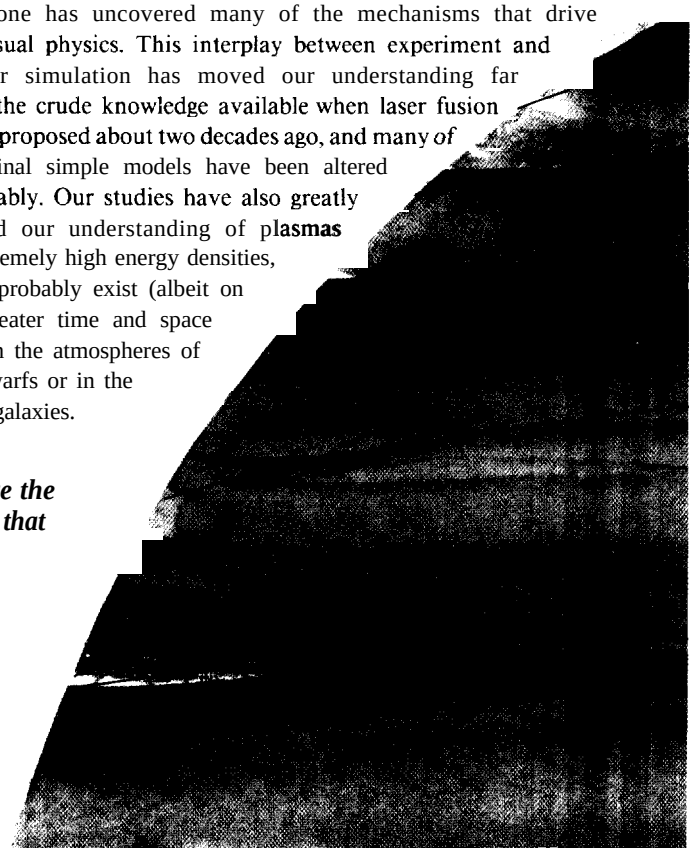

the main actors in the drama of high-energy plasma physics are the intense electromagnetic field of the $C0_2$ laser, the strong magnetic fields that may encircle the laser spot, and the ions driven from the target surface, sometimes, as depicted here, in the form of a highly collimated jet.

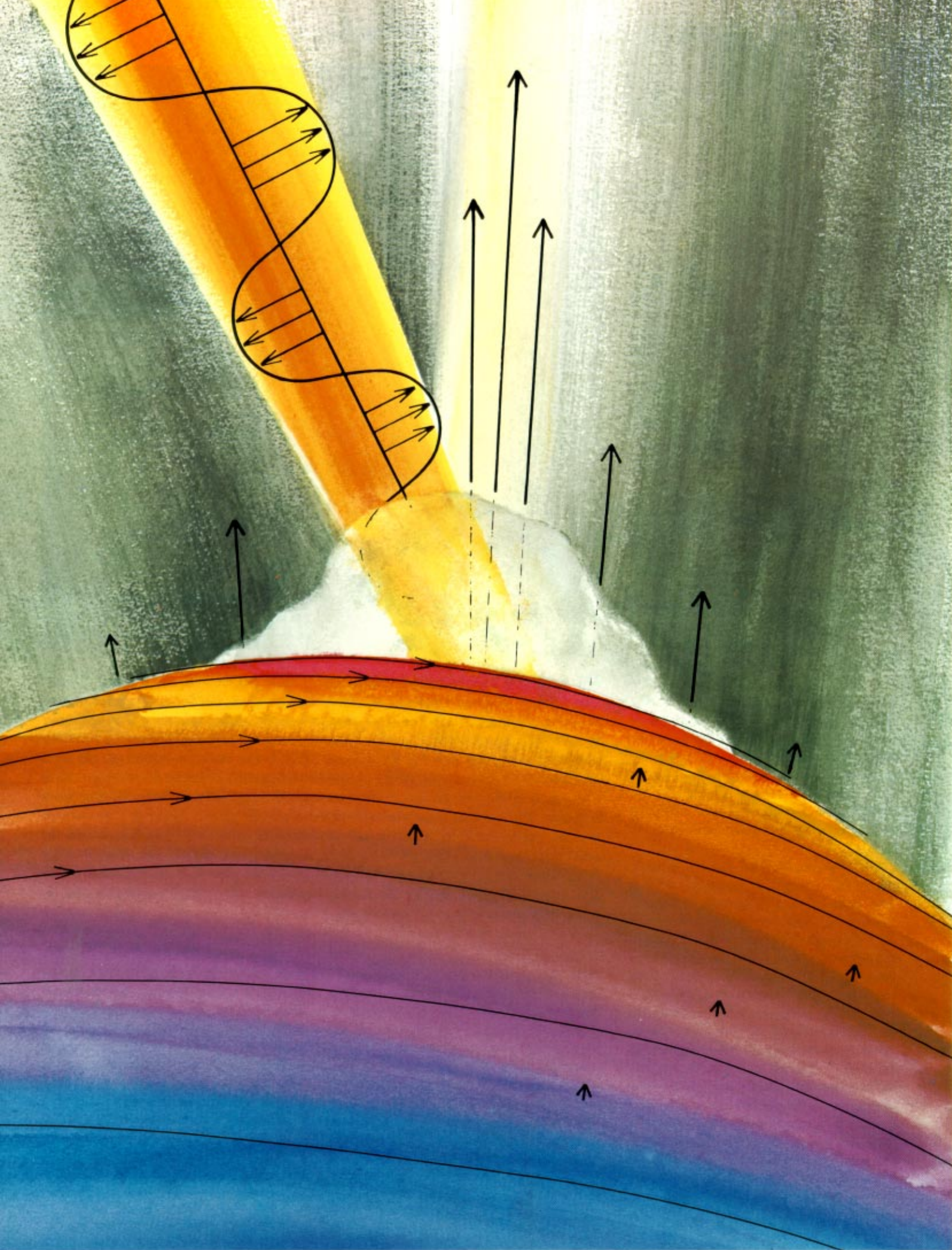

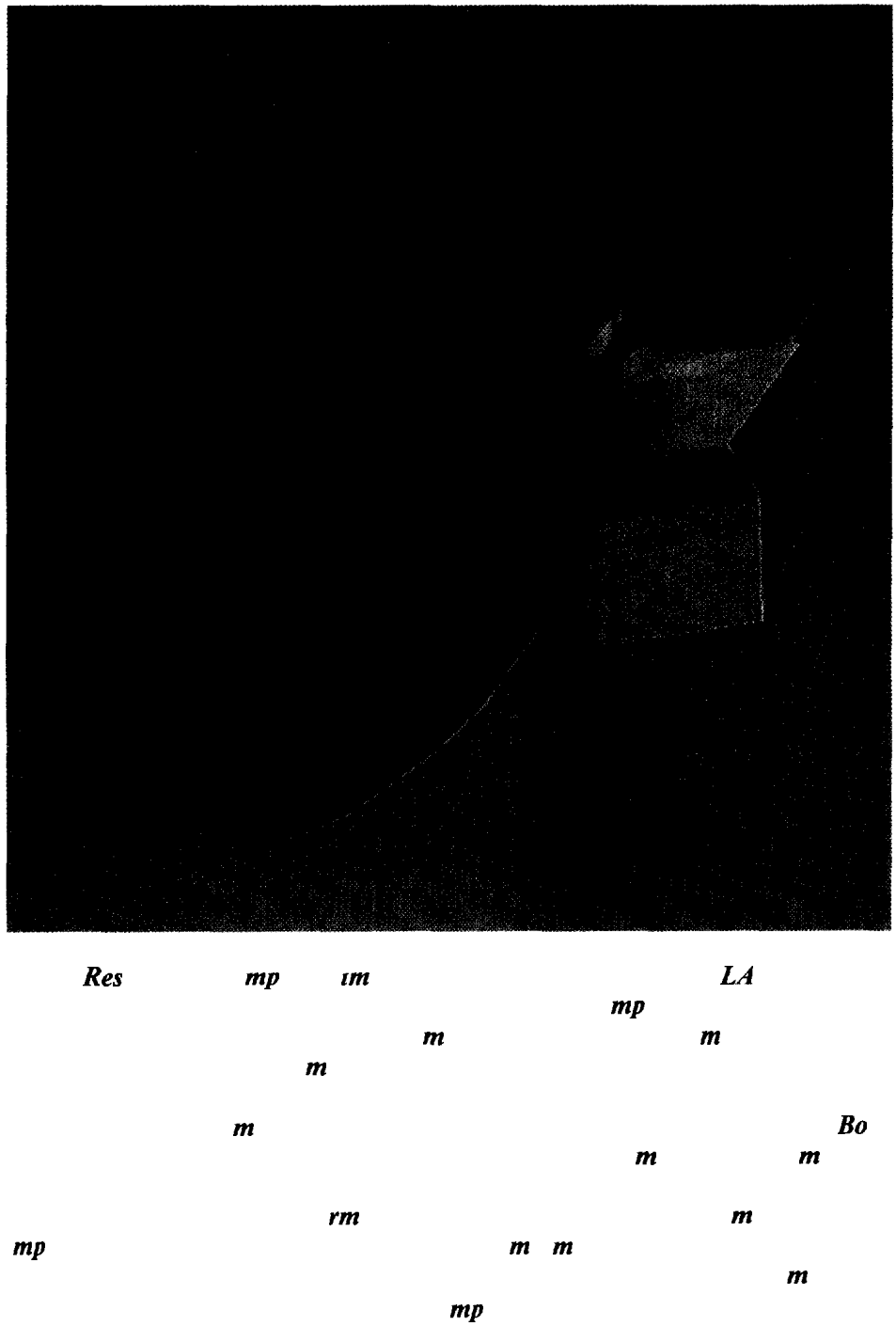

Grafic program developed by Mel Prueitt.)

This article, although noting the difficulties and successes of $C0_2$ laser fusion, concentrates rather on the journey of exploration into a unique state of energy and matter. Within the hot atmospheres of our miniature almost-suns, we have generated phenomena that cannot be easily observed in the laboratory by any other means. Being able to produce such exotica has provided an opportunity to increase our knowledge dramatically about the fourth state of matter. We describe here the current advances achieved because of this opportunity.

Why is the problem of laser fusion so complex? Using the energy of a laser beam to implode microscopic bits of matter requires precise control of a great variety of phenomena. The initial absorption of laser light at the target generates a hot plasma of electrons and ions, which can be likened to the corona surrounding a star. Additional laser light must penetrate this corona and be absorbed efficiently. The absorbed energy must then be transported to the inner layers of fuel in a manner that will produce the desired implosion. Energy that penetrates the target too rapidly preheats the fuel, a highly undesirable effect because it makes the implosion more difficult by greatly increasing the amount of energy needed to compress the fuel.

Vast changes in scale immensely complicate the research. We must deal with at least eight orders of magnitude in density, understanding the physics of matter from 10^{-5} gram per cubic centimeter (g/cm^3) in the tenuous corona where the laser light is absorbed to 10^3 g/cm^3 at the center of the imploding pellet. Distances range from 10^{-5} cm for charge separation in the plasma to 10° cm for the distance that hot ions may be ejected from the target during the laser pulse. In times as short as 10^{-15} second, the electromagnetic fields of the laser light and the plasma change appreciably, yet 10^{-8} second is needed to compress the pellet. Figure 1 shows the range of these three parameters for one computer simulation.

Vast changes extend to other parameters as well. Electrons in the cold pellet with initial energies of less than 0.1 electron volt (eV) may be accelerated in the corona to energies as high as 10^6 eV. If the target is illuminated uniformly and no instabilities develop in the plasma, there will be no strong magnetic fields. However. some of the strongest magnetic fields yet generated in the Laboratory-as high as 10^4 teslas—may surround isolated laser spots.

While the physics of laser fusion discussed here emphasizes the nearly collisionless physics of very hot plasmas, high-density collisional physics at the core of the target must also be understood. We must include the effects of spontaneously generated magnetic fields, the atomic physics of weakly to highly ionized materials, and the effects of these ions and fields on the transport of particles and photons of all energies. Frequently the processes are far from equilibrium, requiring elaborate rate equations for a reasonably accurate description.

Collective Effects. One of the biggest problems for laser fusion has been how to deposit light energy in the target efficiently. The very

properties of lasers that allow production of the extreme high power and intensity needed for fusion can work against a desirable form of energy deposition. In particular, the wave nature, the high coherence. and the narrow bandwidth of the light all contribute to peculiar collective effects in the deposition that reduce the efficiency. It is the highly organized properties of the laser light that tend to drive the hot plasma in the target far from thermodyamic equilibrium, a state with potentially serious consequences. Much of the history of laser fusion is a record of attempts to predict, measure. and avoid the deleterious effects of the coherent properties of the light.

Collective effects arc especially dominant at the CO_2-laser wavelength of 10 μm, whereas, at shorter wavelengths, plasma-light interactions tend to be more collisional. and collective effects are less important. Specifically, the collective effects of $C0_2$ lasers produce *hot electrons* in the corona surrounding the target. These electrons have very high kinetic energies and penetrate the target material quickly. As already pointed out. energy in this form is not favorable for laser fusion.

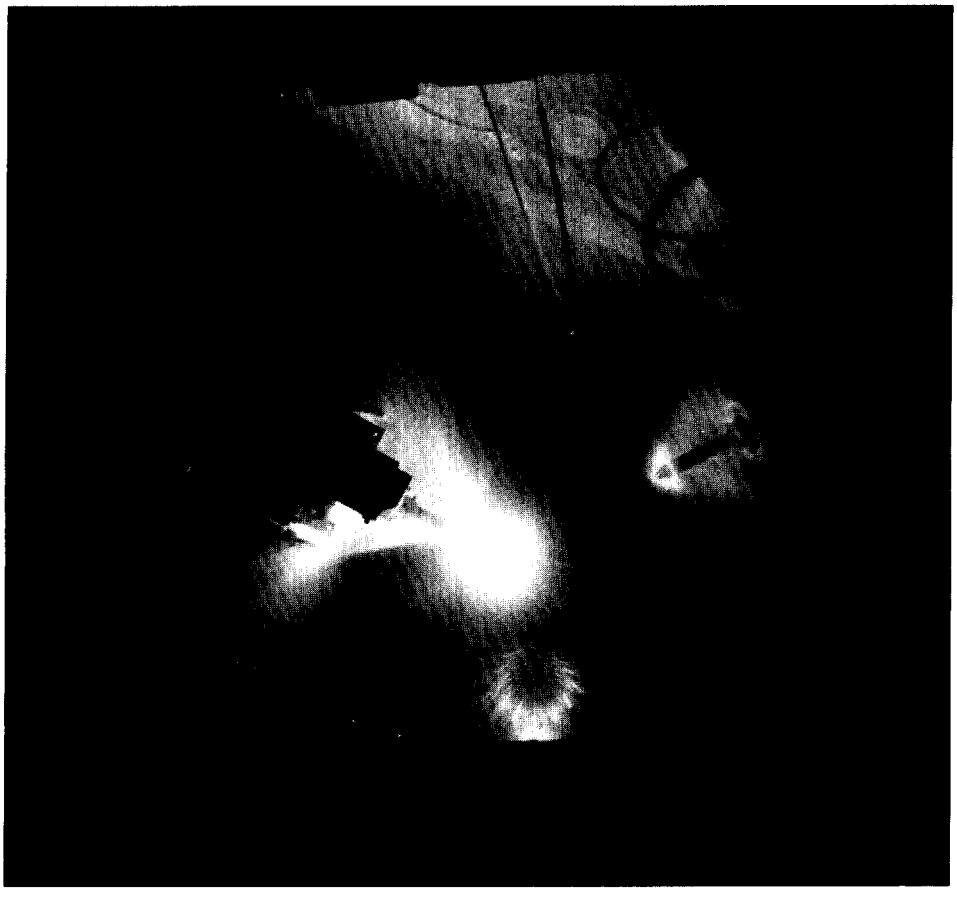

A fusion target bathed in light and plasma during a shot with about 20 kilojoules of energy from Antares. The target is mounted at the end of an insertion mechanism that projects from the left; the object to the right is an x-ray pinhole camera; the circular pattern toward the bottom is a reflection. (Photo by Fred Rick.)

In the early years of research on CO_2 laser fusion, it was thought that the absorption necessary for implosion could only be achieved at high laser intensities if collective absorption processes played a significant role, Simple estimates implied that the temperature, or average kinetic energy. of the hot electrons would be high enough to be potentially harmful. When experiments showed a lower hot-electron temperature than estimated, optimism for long-wavelength lasers increased. Computer simulation models confirmed and explained the experiments. Unfortunately. when more intense lasers and more sophisticated experimental instruments became available. measurements at the higher intensities showed a new, dramatic increase in the hot-electron temperature. Computer simulations at the new intensitites, using more powerful computers not available earlier, again agreed with the experiments.

These latest results have greatly diminished our confidence in the possibility of *long-wavelenght* laser fusion. However, because hot electrons represent an extreme non-Maxwellian distribution of' particles, these experiments are able to generate a variety of interesting and complex plasma phenomena. Here we discuss these phenomema and outline the mechanisms that appear to be important in the interaction of CO_2 laser light with plasmas.

Laser Light Absorption and Transport

When lascr light impinges on a target, the initial effects arc absorption of the light and production of' hot electrons. Then energy flows into and through a variety of energy-flow channels, including magnetic fields, acceleration of energetic ions, brcmsstrahlung emission, microwave emission, and heating of a dense "thermal" plasma. Ultimately, it is the heating of the dense plasma and the resulting ablation of thc target surface that produces the implosion by a rocket-like reaction.

Although our understanding of the later energy-flow processes has been largely empirical, much of our understanding of the initial absorption processes has been theoretical (see "The Tools of High-Energy Laser-Plasma Physics"). This is so because, at the 10-μm wavelength, there are only a lir number of unambiguous experimental signatures that define *specific* absorption processes rather than reflecting an overall effect. As a result. most of the information on absorption comes from computer simulations and analytic theory that have been iterated to reproduce macroscopic experimental data, such as the hot-electron energy spectrum or total absorption. As a result, the analysis has, in fact, been a difficult problem. Fortunately, we have been very successful in putting together a detailed picture of specific absorption mechanisms. What are the main elements of this picture'?

The Critical Density. Initially, the laser light arrives at the target in a near vacuum with the intensity adjusted to achieve nearly uniform illumination. Such uniformity is difficult to maintain, however, because as the target heats up, hot plasma is blown off. and the propagation of light is altered by the changing density of the plasma. In fact, at a certain density called the *critical density* n_c, light does not penetrate further.

In more mathematical terms the index of refraction n of a plasma is given by

$$n^2 = 1 - \frac{\omega_p^2}{\omega^2}, \qquad (1)$$

where w is the laser frequency and w_p is the natural frequency of oscillation of electrons in the plasma. This latter frequency, called the local plasma frequency, is given by

$$\omega_p^2 = 4\pi \frac{n_e e^2}{m} \qquad (2)$$

where n_e, e, and m are the electron density. charge, and mass. respectively.

continued on page 10

The Tools of High-Energy Laser-Plasma Physics

The laser fusion program has considerable strength in both theory and experiment, The complexity of the physics has kept the program at the forefront *in* developing new theoretical tools, experimental techniques, and diagnostics. For example, it is experimentally taxing to measure phenomena on a time scale of picosecond when the entire experimcnt occurs in about a nanosecond and to resolve phenomena spatially at the 1(wavelength of CO_2 light when targets may be as large as millimeters.

In addition, many of the phenomena on the submicromcter, subpicosccond scale—the truly microscopic-strongly influence the macroscopic behavior but can't be readily measured. Computer simulation is then heavily relied on to couple microscopic phenomena to macroscopic observables.

Theoretical Tools

Three codes—WAVE, VENUS, and LASNEX-are used to simulate laser fusion phenomena. As depictcd in the figure, each code simulates phenomena occurring within different ranges of density, time, and space.

WAVE. The code that deals with the most microscopic aspects of energy absorption and transport in the target is WAVE. a 2-dimensional particle simulation code. WAVE is an explicit code that does a first-principles calculation; that is, it solves, in a self-consistent manner. Maxwell's equations and the relativistic Newton's laws for particles in 3-component electric and magnetic fields. WAVE typically advances 10^6 particles on a grid of 10^5 cells for 10^4 time steps.

only a portion of the absorption problem can be modeled by WAVE because the time step must be limited to a small fraction of the period of oscillation of the laser light (that is. a small fraction of about 0.03 picosecond). Thus WAVE can cover only a few picoseconds in a given problem, even with the immense power of the Los Alamos computing facilities. In turn. the grid size of one cell is limited to the distance light travels in one time step. As a result. the code is used primarily to study the details of absorption in the region between the underdense plasma of the corona and the overdense plasma close to the surface of the imploding target. At the very low densities of the underdense plasma,

absorption lengths become too long; the code cannot both have the required cells per wavelength of' light and still span the absorption length. In the overdense plasma the time and space scales are so short that it is impractical to resolve them with WAVE.

Because of such limits to the time and space scales, the initial conditions and the boundary conditions for the fields and particles are unknown and must be put into the calculation separately. Much of the skill in using the code involves estimating these conditions correctly: they should be consistent with themselves, with hydrodynamic calculations, and with experiment.

Why not expand the time scale by increasing the time step? WAVE calculations arc performed by alternately advancing the particles and then the fields. If the time step becomes much larger than a natural frequency in the problem, the calculations can become unstable, The problem is avoided by estimating what the particles *are going to be doing* and then plugging these estimates into the step that advances the fields. This type of code is called *implicit* and forms the basis of our second theoretical tool.

VENUS. Use of the implicit code. VENUS, allows the time and grid size to be increased by about a factor of fifty). Although the increase is obtained by neglecting some high-frequency phenomena. it allows us to handle the spatial scales needed for the study of collective phenomena. In particular, VENUS has been able to verify a model in which very strong self-generated magnetic fields play an important role in electron transport. These magnetic fields also provide the mechanism for copious fast-ion emission, that is, for the ion jets that have been observed streaming from targets. Because of their success with the ICF program, a new generation of implicit codes is rapidly being adopted by the magnetic fusion and space physics communities.

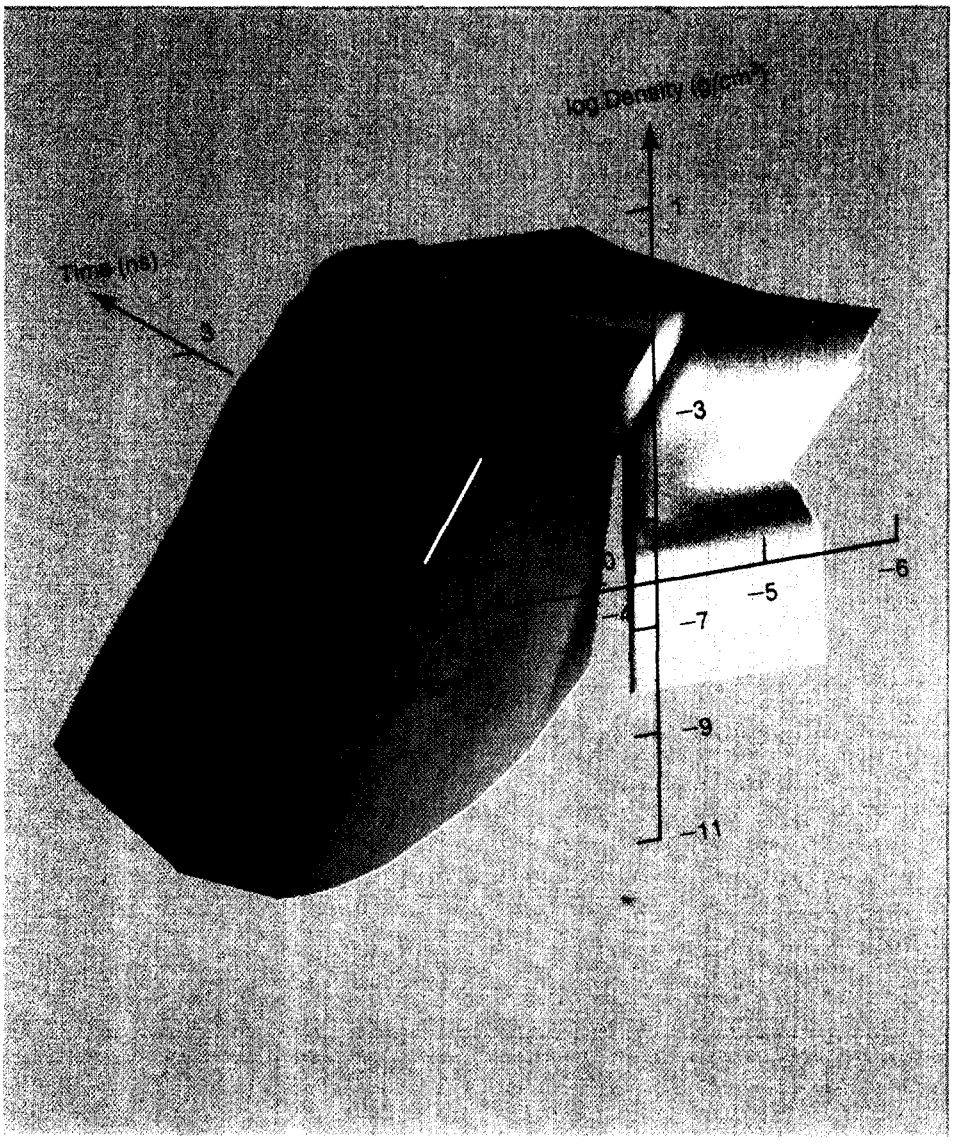

This figure depicts the approximate range of parameters dealt with by each of the computer codes WAVE, VENUS, and LASNEX in typical simulations of laser fusion. The entire surface is a LASNEX calculation, whereas the thin black line on the red surface represents the range of a VENUS calculation, and the even thinner white line represents the range of a WAVE calculation. For ***example, while the LASNEX calculation can span a range of time from O to several nanoseconds, VENUS is confined to a range of only 0.1 nanosecond and WAVE to a range of 0.01 nanosecond.***

Although quantum mechanics and atomic physics are not included in the implicit codes, the fully developed strong turbulence that can occur in laser-plasma interactions is still described accurately. Such descriptions are limited only by the computer resources. In the last decade the scale of accessible problems has increased by a couple of orders of magnitude because of improvements in both computer hardware speed and the numerical algorithms employed in the implicit codes. This increase has greatly broadened our understanding of the physical processes.

LASNEX. The code that deals with phenomena on the largest time and space scales is called LASNEX. This code is a 2-dimensional radiation flow and hydrodynamics code. LASNEX is used to model electron transport. radiation flow, hydrodynamics of' implosion. and possible thermonuclear burn in the target. However. the models in this code arc phenomenological, and the simulation is of relatively macroscopic phenomena.

We can see how these three codes mesh by summarizing the various steps for modeling the production of hot electrons. WAVE generates the initial models for such things as the distribution and energies of the hot electrons, but only in the limited region between the overdense and the underdense plasma. To predict large-scale behavior of the plasma. a model generated by WAVE is used in LASNEX and adjusted to fit macroscopic data. However, the time scale of typical LASNEX calculations is too coarse to resolve electron flow in the underdense plasma with its accompanying generation of magnetic fields, AS a result, the model is incorporated into VENUS to study these important collective phenomena.

The insight gained from using WAVE and VENUS to simulate and verify models has led to two important improvements for LASNEX. The various physics packages used in the code have been improved, and a better choice of input conditions to the code is possible.

Experimental Tools

A wide variety of experimental techniques have provided the basic data against which the theoretical models must be compared.

Absorption and Energy Flow. We obtain the overall energy delivered to a target in one of' two ways. The scattered 10-yin light not absorbed by the target can be measured directly with in infrared-sensitive detectors and subtracted from the incident energy. Or all of the ion, electron, and x-ray energy emitted from the target can be measured using calorimeters that are gold-coated to reflect, and therefore reject, scattered CO_2 radiation.

To determine the ho-electron temperature and the amount of hot-electron energy, we can measure either electron or x-ray spectra. Although hot electrons from the target can be detected with magnetic electron spectrometers, only a few electrons actually manage to escape. Therefore, the bulk of the electron energy is studied by measuring the bremsstrahlung radiation resulting from collisions of hot electrons with atoms in the solid parts of' the target. We measure these hard x rays with a multichannel broadband x-ray spectrometer that uses an array of filtered scintillators coupled to visible light photodiodes. The measurement covers the spectrum from about 30 kiloelectron volts (keV) to large fractions of an MeV with nanosecond resolution. One detector that responds to x rays of energics greater than 100 keV is used to study the time history of the hot-electron energy with subnanosecond resolution.

The target. heated by hot electrons, emits soft x rays (below 1 keV). This radiation is detected with separate multichannel spectrometers that have filtered vacuum photodiodes sensitive to soft x-ray illumination. The diodes arc electrically designed for fast response and are coupled to ultrafast oscilloscopes (developed in the nuclear weapons program), providing a time resolution of better than 300 picoseconds.

Spatial details of the intensity or energy of the x rays from the surface of the target are resolved with multichannel x-ray collimators that restrict the field of view of' the diodes. Although such collimators arc simple in principle, the small targets used in the lascr fusion program require that the collimating pinholes be machined and positioned precisely. To achieve the required 25-pm accuracy, the pinholes, only 150 μm in diameter, arc aligned with respect to the target and to each other with optical techniques.

The total absorbed energy measured with ion calorimeters, the fast-ion energy obtained with filtered calorimeters, the energy deposited in the target as determined from the hard x-ray bremsstrahlung emission, and the target surface temperature obtained from soft x-ray measurements, all help reveal the overall energy flow, in the experiment. The comparison of these related measurements has provided considerable information about the basic physics of plasmas created by $C0_2$ lasers. However, considerably more detailed information is required if the physics is to be understood on a more fundamental, microscopic basis.

High-Resolution Imaging and Spectroscopy. Optical and x-ray emission can be imaged, with simple optical or pinhole cameras, to map thc distribution either of hot electrons in the target or of the beating of the corona. These techniques can identify nonuniformitics in energy deposition due to imperfections in the laser beam or to plasma effects. By using film and filter combinations

to compare images of x rays at fractions of a keV with images of x rays in excess of tens of keV, a picture of the hot-electron flow can be built.

Crystal or grating spectrographs are used to obtain high-resolution x-ray and vacuum ultraviolet spectra that offer a wealth of information on the details of the atomic physics of the plasma, as well as on the plasma conditions themselves. For example, we can identify plasma parameters, such as temperature and density, by selecting specific x-ray transitions from elements in the target and then examining the relative intensities of x-ray lines from different ionization stales, as well as for lines from a single ionization state. Spectral line broadening and detailed lineshapes relate to the density of the plasma surrounding the emitting atom. Particularly in the case of extreme conditions far from thermodynamic equilibrium, line intensities and lineshapes must be compared to detailed atomic physics codes to yield accurate temperature and density information. Such information is very useful for evaluating the conditions of the imploding fuel.

Specific characteristic x rays can give us further important information. For example. hot electrons have enough energy to create inner electron shell vacancies, giving rise to K-1ine x rays, but thermal background electrons do not have enough energy. Therefore, we can image the target in K-line radiation and track the flow of hot-electron energy. We can do this by using two pinholes in a single pinhole camera with specially matched filters: one passes the light of the K line and one does not. By subtracting one image from the other, wc can build. in effect, a single-wavelength image of the target. A more attractive, state-of-the-art solution is to use the so-called layered synthetic microstructure (LSM). The LSM acts like a crystal in that it reflects, in accordance with its designed lattice spacing and Bragg's law, only selected frequencies. Placed between the pinhole and the film, the appropriate LSM can be used to reflect only the transition of interest.

Microfabrication techniques can be used to place materials at strategic locations in the target, for example, in a spot on the target surface or as a thin layer on or beneath the surface. The x-ray emission from these materials then serves as a tracer, allowing us to determine the amount or the time of energy flow to thcse locations by observing the spectral lines characteristic of the tracer material. This technique also allows us to examine in detail the plasma conditions of a well-defined region; we don't have to be content with averages over all densities and temperatures in the plasma.

In addition, both images and spectra can be time resolved to less than ten picosecond with optical or x-ray streak cameras, enabling us to follow the evolution of the plasma as the experiment proceeds. For example, optical streak cameras, filtered to record only one of the high harmonic frequencies of the CO_2 light, can determine if the conditions producing such harmonics are present throughout the nanosecond experiment. On the other hand, infrared optical emission (for example second harmonic emission from the steep density gradient, light reflected from the critical-density surface in the plasma, light that is Brillouin scattered near 10 μm, or light that is Raman scattered at longer wavelengths) must be measured with fast infrared sensors and spectrometers. Because there is nothing equivalent to a streak camera sensitive to these low-energy photons, it is difficult to examine, in the detail we would like, the evolution of these signatures of the absorption process.

Many of these instruments-particularly the x-ray pinhole cameras, spectrographs, and collimators—must be close to the target and must survive the blast of particle debris and intense x-rays from each shot. In a typical Antares shot hundreds of gigawatts of hard x rays and gigawatts of microwaves arc emitted. Heroic measures are required to shield detectors, film, and electronics sufficiently to make the necessary measurements.

The wide range of measurement techniques we have used in this hostile environment, combined with our ability to modify target design in a microscopic manner, has allowed us to develop a detailed empirical base against which the theoretical picture can be compared.

Comparison with Experiment

The code that provides the most direct link with experimental data is, of course, LASNEX. With its post processing packages, LASNEX can simulate directly the outputs of such diagnostic records as pinhole photographs and streak camera images, as well as bremsstrahlung, ion emission. and soft x-ray emission spectra.

The code also calculates the source spectra and so can be used to help deconvolute experimental data. For example, it can extract the electron temperature from the hard x-ray bremsstrahlung spectrum or extract the compressed fuel properties from the x-ray pinhole images and x-ray spectra. Using the code to model a variety of phenomena simultaneously on a given target shot greatly enhances our confidence that we understand the target behavior.

Matching the experimental data frequently requires an iteration in the input conditions to LASNEX, and often the search for a specific signature of a phenomenon predicted by the code leads to suggestions for modifying existing diagnostic techniques or developing new ones. From this interplay between theory and experiment new target concepts are developed that might better use the energy flow. ■

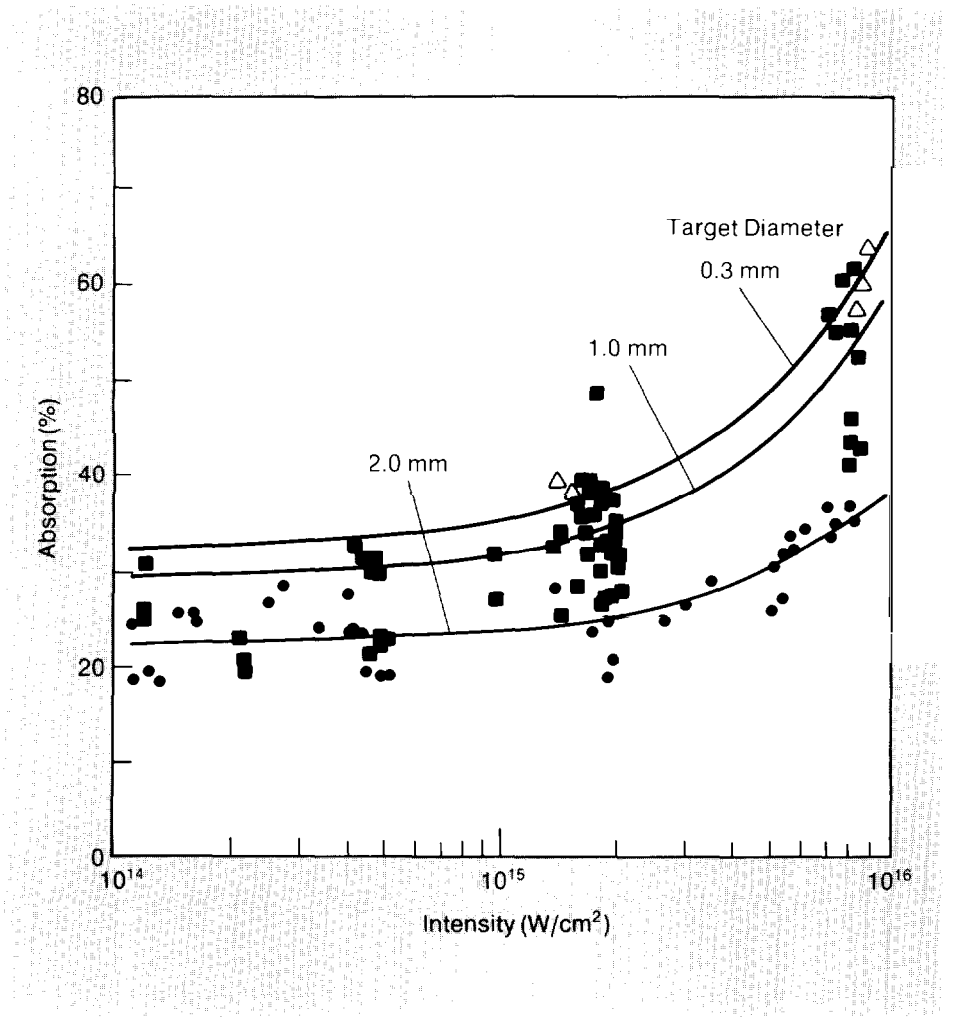

Fig. 2. Absorption of Helios CO_2 laser light on spherical gold targets of various diameters as a function of intensity. The targets were illuminated symmetrically by eight laser beams, and the absorption was measured with fourteen calorimeters deployed around the target chamber, each sensitive to particle and x-ray fluxes but not to scattered 10-pm laser light. The decrease in apparent absorbed energy with larger target diameter is attributed to ion jets that are more directional, returning toward the focusing mirrors and missing the calorimeters. For small targets ion emission is more isotropic.

We see from Eqs. 1 and 2 that as the plasma density n_e increases, so docs the plasma frequency w_p until eventually w_p becomes greater than the laser frequency w and the index of refraction becomes imaginary. At this point, light will penetrate no further and is reflected, making this the critical density surface. The region of the plasma with density very close to n_c plays an important role in the absorption mechanisms to be discussed because it is here that the laser and plasma frequencies essentially match $(w = w_p)$.

How much of the incident light is absorbed? Fig, 2 shows the absorption on spheres of various sizes as a function of Helios CO_2 laser intensity. Typically, at lower intensities the absorption is about 30 per cent, whereas it can exceed 60 per cent at higher intensities,

Our description of the absorption processes will start with the simplest form of absorption, inverse bremsstrahlung. This is the dominant absorption mechanism only at low intensities. For higher intensities we have to invoke more complex mechanisms—in particular, those resulting from collective effects. However, the main features of inverse bremsstrahlung form a necessary introduction to the other mechanisms.

Inverse Bremsstrahlung. Inverse bremsstrahlung is a result of collisions between electrons and background ions. Electrons oscillating in the laser electric field scatter randomly off the ions, absorbing a photon of laser light in the process. Thus. the coherent oscillation energy of the laser is converted into the random kinetic energy of electrons.

The rate at which energy is lost from the laser field by inverse bremsstrahlung is approximately equal to the rate at which the electron plasma is heated, Equating these two rates leads to an expression for the dependence of the damping rate v_p of the laser field on the electron-ion collision frequency V_{ei}:

$$\nu_D = \nu_{ei} \frac{n_e}{n_c} . \qquad (3)$$

Because v_{ei} is the frequency for classical Coulomb collisions. it is proportional to $T_e^{-3/2}$, where T_e is the electron temperature. Thus, the efficiency of inverse bremsstrahlung will *increase* as electron temperature *decreases.* In other words, inverse bremsstrahlung preferentially heats low-energy electrons, keeping the plasma close to thermodynamic equilibrium.

How does absorption by inverse bremsstrahlung depend on the wavelength of the laser light? At a specific density, long-wavelength light is absorbed more efficiently than short wavelengths. However, the sharp increase in plasma density encountered by the light as it moves through the corona toward the target reverses this dependence.

First, as suggested by Eq. 3, most of the incident laser light is absorbed near the critical density surface where $n_e = n_c$. But Eqs. 1 and 2 show that n_c, and thus the position of n_e in a density gradient, will be different for different wavelengths. In fact,

$$n_c \propto \lambda^{-2} , \qquad (4)$$

which means that shorter wavelength light penetrates further. encountering electron plasma that is both denser and cooler. These features increase the absorption efficiency for short wavelengths.

A second consideration is the thickness of the region of the plasma that is absorbing significant amounts of light. The sharper the density gradient. the thinner the region between outer, underdense corona and the reflecting surface beneath. A measure of this sharpness is the *density scaleheight L,* the distance over which the density drops by a factor of *1/e.* Also, the absorption length for light, which is proportional to the wavelength λ, must be taken into account. If these parameters arc incorporated with the energy-balance considerations that led to Eq. 3, we find that significant absorption occurs only for intensities, in watts per square centimeter (W/cm^2). of

$$I < 5 \times 10^{14}\, ZL/\lambda^4 , \qquad (5)$$

where Z is the ion charge state, *L is* in cm, and λ is in μm.

For example, in CO_2-laser-fusion experiments with gold targets. Z is typically less than 79, λ is 10 μm, and the density scaleheight *L* might be as large as 0.1 cm. which corresponds roughly to the distance the underdense plasma expands in a nanosecond. Such numbers show that absorption of CO_2 laser light by inverse bremsstrahlung is negligible at intensities above $10^{12}\ W/cm^2$, an intensity lower than that at which any of the data of Fig. 2 were obtained. Essentially, the electron-ion collision rate is too slow to account for the amount of energy actually absorbed at the intensities of interest.

The dependence of bremsstrahlung absorption on wavelength (Eq. 5) was well known before any experiments or simulations had been performed. Although research has revealed effects that modify the k^{-4} relation, the basic conclusions remain the same. To be able to use the CO_2 laser for laser fusion, one must depend upon collective effects. In contrast, for the shorter wavelengths of visible and ultraviolet lasers, such as the KrF laser, inverse bremsstrahlung dominates the absorption process. Forms of collective absorption are present. but only to a modest extent.

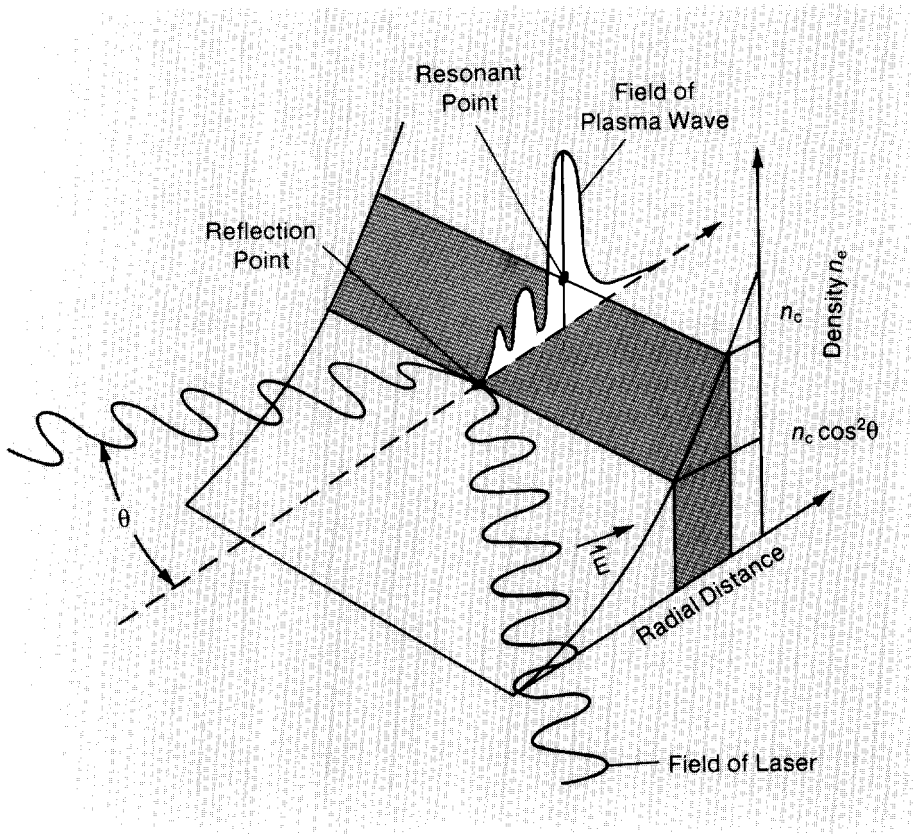

Fig. 3. Resonant matching absorption. The sinusoidal line represents the electric field E of laser light oscillating at frequency w. The sloping surface represents a density gradient in the plasma that increases toward the target. Because the light is oblique (at angle 0), it is reflected when the density of the plasma reaches $n_c \cos^2 0$. Oblique light also has a component of its field perpendicular to the surface, and that part of the field can tunnel inward to couple with the longitudinal electrostatic field of the plasma wave. This coupling occurs most efficiently at the resonant matching point, that is, the point where the plasma density equals n_c and the plasma frequency w_p, equals w. The steeper the density gradient, the smaller the gap between the reflection and resonant matching points and the more efficient the absorption.

Two basic absorption mechanisms involving collective effects have been identified as important: resonant absorption and parametric instabilities. Both mechanisms are at work in all laser plasma interactions but arc particularly prominent at the wavelength of the CO_2 laser. Also, both are a result of the pressure of the incident light wave, the so-called *ponderomotive force.*

This important low-frequency force is proportional to the light intensity and the density ratio n_e/n_c. For example, at the intensity of $10^{16}\ W/cm^2$ achieved at Antares. the pressure of the light at its reflection point is about 5 megabars. Such a large force is able to distort the flow of expanding plasma at low densities. It is thus responsible f-or most of the instabilities induced by the incident radiation in the outer layers of underdense plasma and plays a critical role in the collective absorption mechanisms.

A Mechanism for Moderate Intensities: Resonant Absorption

The first collective absorption mechanism, resonant absorption, is a *linear* coupling of the electric field of the laser beam to *longitudinal electron-plasma waves.* This coupling will not occur unless the electric field of the light has a component parallel to the density gradient. Thus. the light must be oblique to the surface of the plasma (Fig. 3).

An electromagnetic wave with incident angle θ is reflected *not* at the critical density n_c but at the lower density $n_e = n_c \cos^2\theta$. If

the absorption is to be efficient, the light must reach the resonant-matching point at n_c where $w = w_p$. In plasma with a steep density profile, these two points are close together, and a significant part of the wale may tunnel quantum mechanically to the resonant-matching point. Once there, the component of the electric field vector that lies along the density gradient induces density fluctuations at the local plasma frequency w_p. This coupling acts as a source of plasma waves, extracting energy from the incident electromagnetic wave.

The efficiency with which resonant absorption converts light energy to plasma-wave energy depends sensitively on the incident angle and the length of the gap between the reflection point and the resonant-matching point. For example. simulations show that at a typical angle of incidence of' 20 degrees, this length must be *less than a wavelenght of light* to obtain an absorption greater than 20 percent, If the ponderomotive pressure is large, the reflecting light and the locally generated plasma wave together produce a sharp density gradient in the region. In other words, the pressure of the light creates a sudden wall in the plasma that keeps the length short. This allows resonant absorption to be an effective process.

Figure 4, a simulation using our WAVE code, illustrates the enormous density gradients that can be produced. At the peak of the gradient, the density has increased to sixty times critical density with most of this increase happening over a distance of only 1 ›r 2 μm!

Although resonant absorption is a linear coupling between electric field and plasma wave, the gradients involved are so extreme that nonlinear phenomena abound. In fact. resonant absorption at high laser intensities is identified experimentally by a nonlinear phenomenon: the emission of second harmonic light (Fig. 5). How does this occur?

If laser energy is coupled resonantly into the plasma wave, density fluctuations begin growing that cause the index of refraction of the plasma to also change with frequency *w*.

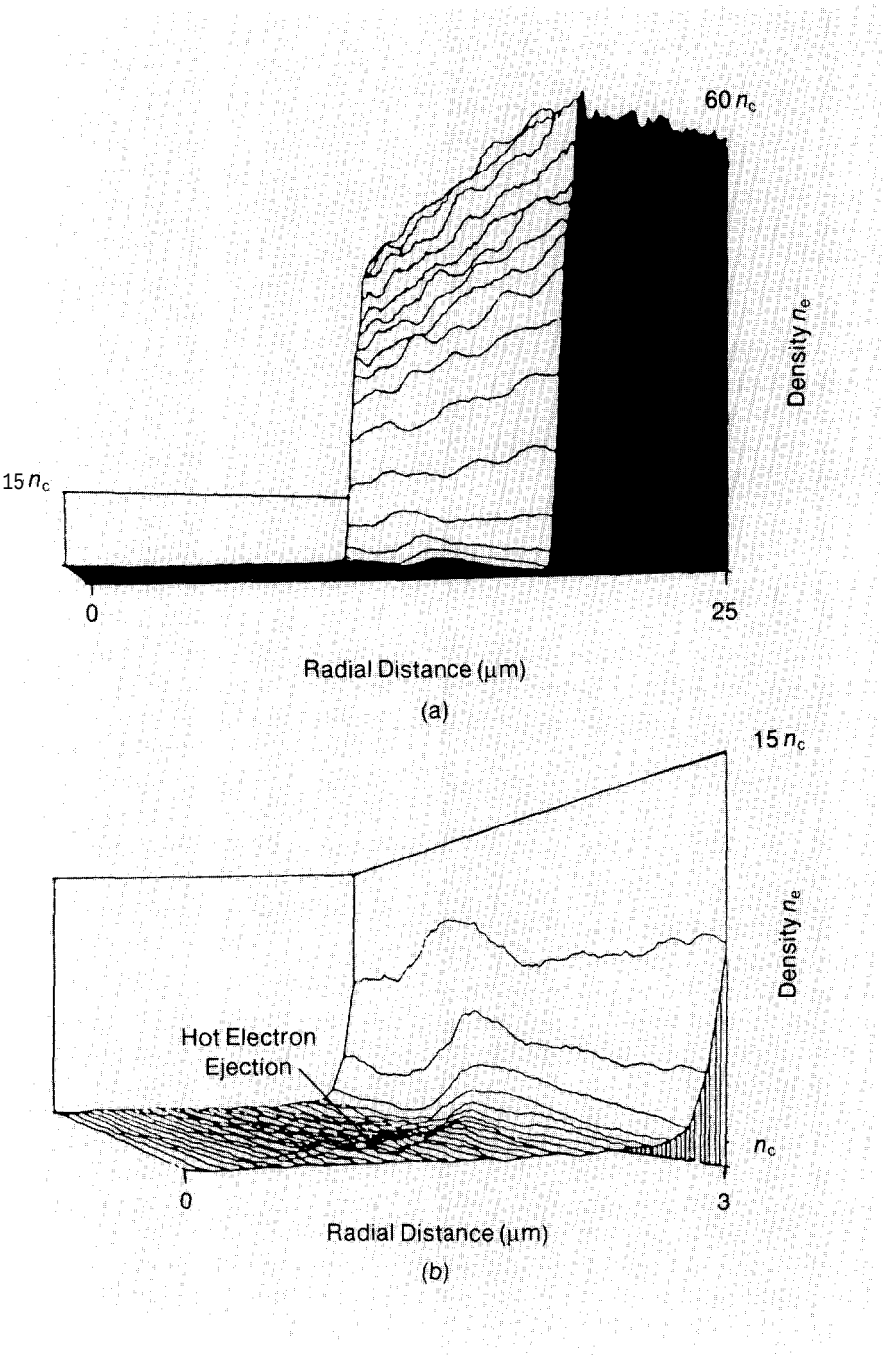

Fig. 4. A calculation by WAVE of the density n_e of electrons in the plasma close to the critical density surface n_c. (a) The density gradient rises to a peak value sixty times n_c over a distance of only a few micrometers. (b) This detail shows a stream of hot electrons being ejected from the surface of the density front.

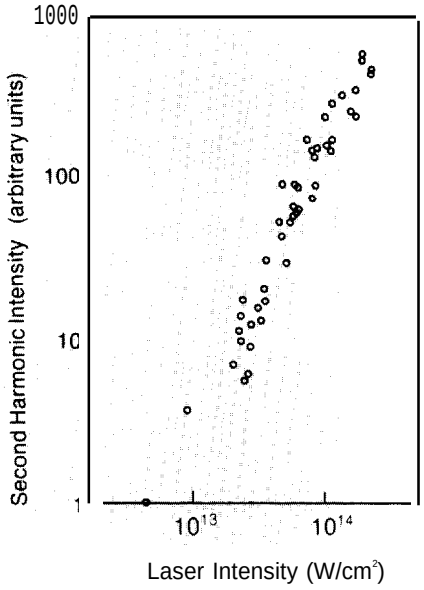

***Fig. 5. Second harmonic emission as a function of the intensity of incident laser light at the target. This emission is experimental evidence for resonant absorption and a sharp density gradient in the plasma. (Adapted from H. A. Baldis, N. H. Burnett, G. D. Enright, and M. C. Richardson,* Applied Physics Letters 34(2979): 327-9.)**

The incident light interacts with this modulated index in a nonlinear or enharmonic manner, generating light at the second harmonic frequency *2w*. The intensity of the second harmonic is proportional to both the incident light intensity and the plasma wave intensity and is thus a direct measure of the amount of energy in the plasma wave.

Wave Breaking. Once energy is placed into the plasma wave by resonant absorption, a number of mechanisms quickly dissipate the energy throughout the plasma. In particular, hot electrons are generated that are shot outward from the sharp wall formed by the density gradient (Fig. 4(h)). What produces these electrons and how energetic will they be?

The primary mechanism is a process known as wave breaking that is analogous to a surfer riding a wave, only here it is an electron riding a plasma wave. In wave breaking only a few electrons arc accelerated by the plasma wave and only over distances of less than a micrometer. However. these few electrons gain energies of hundreds of keV in less than one laser cycle (about 10^{-14} second), becoming the hot electrons.

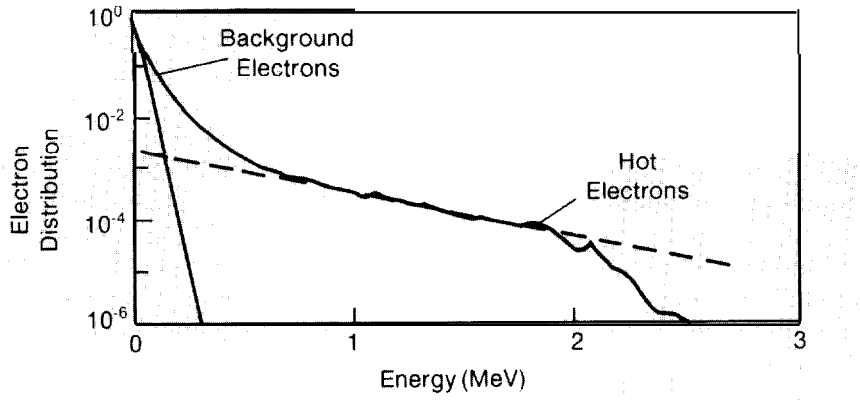

Fig. 6. This calculation with WAVE of the energies of electrons clearly shows two components: large numbers of cooler background electrons and small numbers of hot electrons distributed over a wide range of energies. Even though the hot electrons are few in number, they carry essentially all the energy deposited in the plasma by resonant absorption.

The energy gained by electrons via wave breaking is proportional both to the electric field in the plasma wave and to the *width* of the plasma wave. Although a steepened density profile increases the efficiency of resonant absorption. it also causes that absorption to occur in a physically narrower region of the plasma, generating a narrower width for the plasma wave and reducing the energy of the accelerated electrons. In other words. this effect should make the hot electrons generated by resonant absorption somewhat cooler than originally thought.

Initial experimental evidence that showed the scaling of hot-electron temperature with intensity to be much weaker than expected spurred a detailed exploration of the effect with simulations and experiments. The theoretical results can be summarized by looking at the scaling predictions with respect to intensity I and wavelength λ. Before the studies, it was thought that hot-electron temperature would scale as $I\lambda^2$. Afterwards, it was thought that the temperature would scale as $(I\lambda^2)^{1/3}$: that is, the production of highly energetic electrons would be much less dependent on laser wavelength. This result implied that resonant absorption could help achieve the needed conditions for CO_2 laser fusion.

What else did computer modeling predict? Although wave breaking is a coherent acceleration process, there is a small random change in the acceleration from cycle to cycle. This stochastic clement produces a near Maxwellian distribution of hot electrons. but the region in the plasma where significant wave breaking occurs is very thin. In the larger region of lower density plasma the fraction of electrons that get accelerated is small. The result, overall, is plasma that typically has two components: one component consists of a large number of cooler background electrons. and the other consists of a small number of energetic electrons spread over a broad energy spectrum. Despite their small numbers, it is the hot electrons that carry most of the energy.

A WAVE calculation of the distribution of electrons at high intensity is shown in Fig. 6.

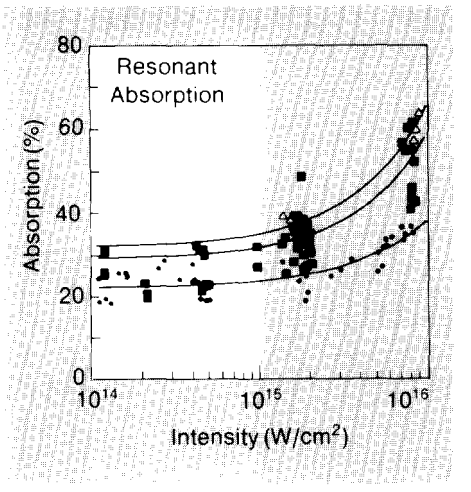

Fig. 7. Resonant absorption explains the almost constant absorption observed for intensities from 10^{14} to 10^{15} W/cm^2.

A major uncertainty in such a calculation is the value of the cool background temperature. We cannot use WAVE-our most rigorous simulation code—to determine this temperature self-consistently, because the temperature depends on the radiative cooling processes. the expansion of the solid material, the ionization rates, and so forth. Nevertheless, wave breaking can be modeled in a relatively simple way with our LASNEX code, and such modeling provides a reasonable match to experiment.

What *is* the match to experiment? First, theory predicts the nearly constant absorption of 20 to 30 per cent observed at intensities from 10^{14} to 10^{15} W/cm^2 (Fig. 7). Further, *at these intensities* scaling with wavelength is weak: that is, a large number of measurements of hot-electron temperature from x-ray emission and ion emission are consonant with the predicted $(I\lambda^2)^{1/3}$ dependence (Fig. 8). At lower intensities, steepening of the density profile is weak, and the original strong scaling holds.

The observation of high harmonics of the incident laser light is our most spectacular confirmation of wave breaking and the steepness of the density gradient. Put simply, the incident laser energy, strips electrons from the density gradient wall in the plasma (Fig. 4(b)). generating many harmonics because of the highly nonlinear nature of the process. One might say that incident light is pressing at the density gradient in a manncr analogous to fingernails scraping across a blackboard. More than thirty-five harmonics of the incident light have been detected experimentally in the scattered light (Fig. 9). confirming the presence of the steepened density gradient.

Figure 10 illustrates the anharmonicity that gives rise to these high harmonics. An electron, attempting to oscillate at the plasma frequency within the thin region of the sharp density gradient, sees a highly asymmetric environment. It moves from low to high density, from a region of low restoring force to one of high restoring force, experiencing extremely enharmonic acceleration. In effect, the electrons of the plasma wave see a restoring force that is essentially proportional to ω_p^2.

How many harmonics should we observe? The highest plasma frequency equals the frequency of the maximum harmonic that gets scattered. Because the highest plasma fre-

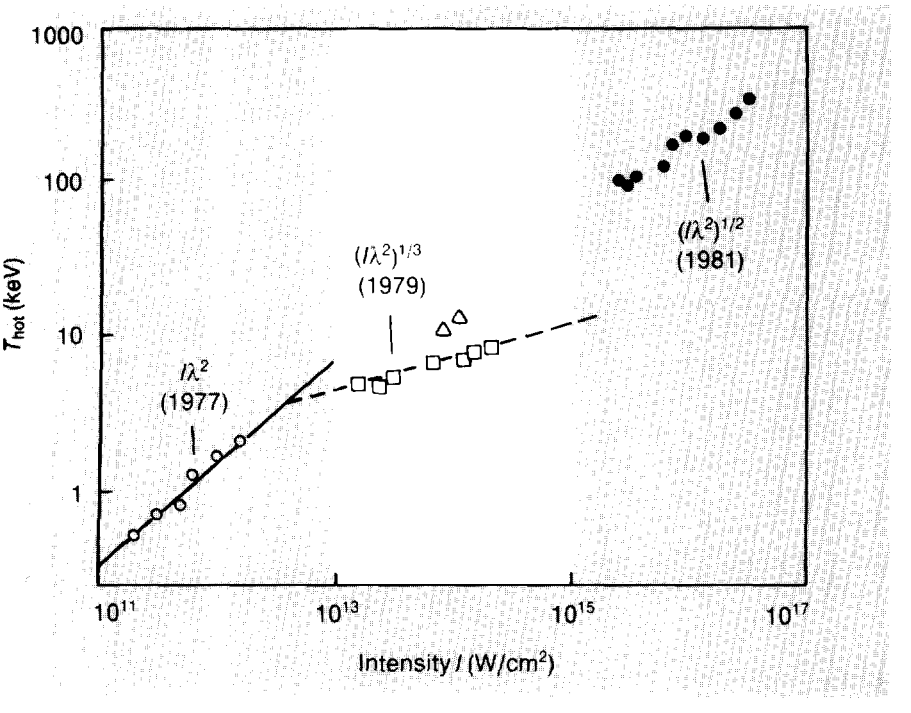

Fig. 8. As the intensity I of the light increases, measurements of hot-electron temperature show different $I\lambda^2$ dependencies, where λ is the wavelength. In 1977 the low-intensity hot-electron temperature scaled as $I\lambda^2$. About that time fast-ion data indicated a weaker scaling at higher intensities, motivating calculations that showed a weaker scaling for T_{hot} in a steepened density profile. By 1979 x-ray data at higher laser intensities was published that revealed the scaling to be proportional to $(I\lambda^2)^{1/3}$, that is, consonant with resonant absorption in a density profile steepened by the ponderomotive force. These results encouraged researchers to think the hot-electron temperature might not be too serious an impediment to laser fusion. The most recent data, at even higher intensities, show a scaling that is proportional to $(I\lambda^2)^{1/2}$. Besides increasing the difficulty of CO_2 laser fusion, these last data imply the onset of another absorption mechanism. (The data in the figure are taken from: C. Stenz C. Popovics, E. Fabre, J. Virmont, A. Poquerusse, and C. Garban,* Le Journal de Physique *38 (1977):761; D. W. Forslund, J. M. Kindel, and K. Lee,* Physical Review Letters 39 *(1977):284 (which cites further original data sources); G. D. Enright, M. C. Richardson, and N. H. Burnett,* Journal of Applied Physics 50 *(1979):3909; and W. Priedhorsky, D. Lier, R. Day, and D. Gerke,* Physical Review Letters *47 (1981):1661.)

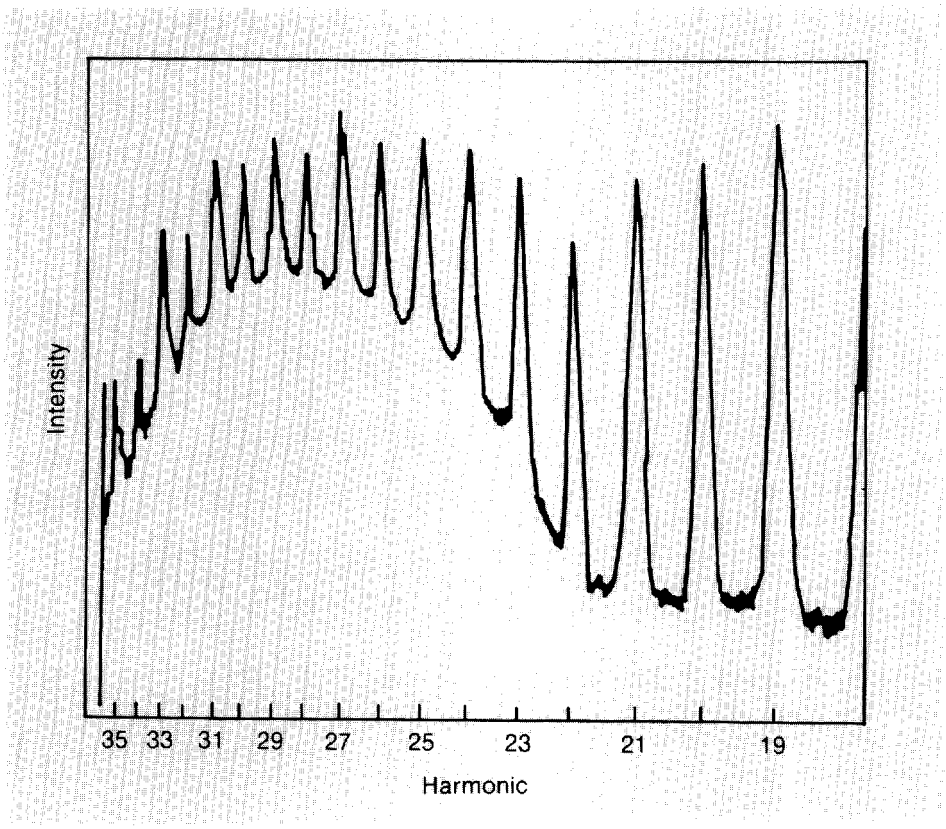

Fig. 9. Harmonics of the laser light frequency w are experimental evidence for a steepened density gradient and acceleration of electrons by wave breaking. The highest harmonic, here 35w, is a measure of the height of the upper density shelf (see Fig. 10).

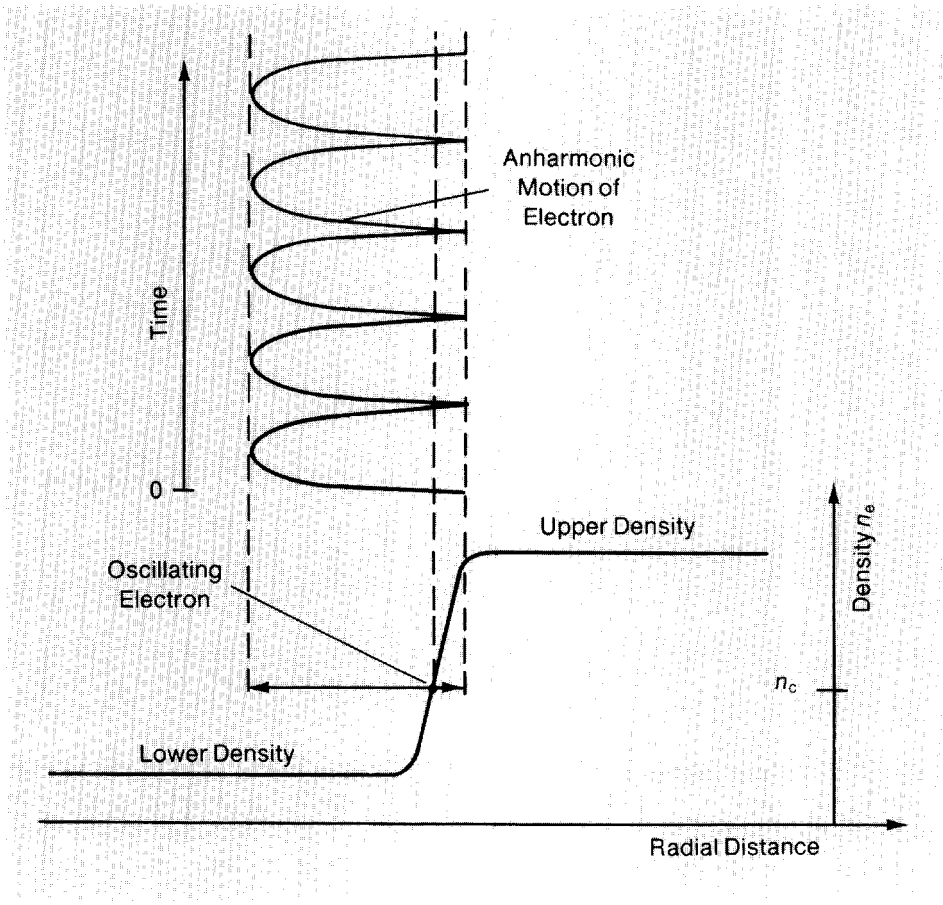

Fig. 10. An electron oscillating within the thin region of the sharp density gradient undergoes extreme enharmonic motion, experiencing a restoring force that is essentially proportional to ω_p^2. The result of this anharmonicity is the generation of scattered light containing the higher harmonics nw of the laser frequency (Fig. 9). The highest plasma frequency—w_p in the upper density shelf—determines the highest possible harmonic frequency. Because the density of the plasma is proportional to ω_p^2 (Eq. 2), the density of the upper shelf is proportional to the square of the highest observed harmonic. Thus, the observation of the 40th harmonic implies a density for the upper shelf that is 1600 times n_c.

quency occurs at the highest density, the maximum harmonic should equal w_p in the upper density shelf. Since $\omega_p^2 \propto n_c$ (Eq. 2), the square of the highest harmonic is a measure of the density in the upper shelf. We have observed close to 40 harmonics. implying that the plasma wave is seeing densities up to 1600 times critical density, that is, essentially solid density.

In recent years both experiments and more extensive calculations have indicated that the very steep density gradient may dissipate quickly. Ultrafast optical streak cameras show that the high harmonics last only during the rise time of the laser pulse. about 200 picosecond. Such transient behavior is due. in part. to the outward expansion of high-density plasma, which eliminates the enharmonic environment that the plasma wave sees.

In addition, experiments above 10^{15} W/em^2 showed that absorption increased dramatically (Fig. 11), contrary to the prediction of a nearly constant coefficient for resonant absorption, and that hot-electron tem-

perature scaled as $(I\lambda^2)^{1/2}$ rather than $(I\lambda^2)^{1/3}$ (Fig. 8). These facts and the short lifetime of the density gradient suggests that an additional absorption process—another type of collective mechanism—occurs at these high intensities.

High-Intensity Absorption and Parametric Instabilities

Resonant absorption involves a *linear* coupling of light to the plasma wave. Parametric instabilities, on the other hand. result from a *nonlinear* coupling with plasma waves. As before, the coupling is through the ponderomotive force, but now light couples to plasma wave frequencies *different* from the resonant frequency.

In general. the conditions for a parametric instability are met when the frequency of a scattered wave w_s, the laser frequency w, and the plasma frequency w_p satisfy conservation of energy,

$$\omega_s = \omega - \omega_p , \qquad (6)$$

and the wavevectors k_s, k, and k_p satisfy conservation of momentum.

$$k_s = k - k_p . \qquad (7)$$

In essence, part of the energy of the laser light appears in the plasma as an oscillating motion of particles-either in electron-plasma waves or in ion sound waves. The remaining energy may appear as scattered light or as another plasma wave, but, in either case. it will be at the lower frequency w_s.

One concern about this type of mechanism is that a significant fraction of the laser energy may be backscattered away from the target as light at frequency w_s. However, as we will explain in a moment, a more serious concern is the generation of very energetic hot electrons.

In general, parametric instabilities occur in the underdense plasma farther out than the critical density surface (Fig. 12). That this should be the case is obvious from the fact that the plasma-coupling frequency w_p is necessarily lower than w, so the matching must occur in plasma of lower density than n_c. The effect then is to reduce the energy of' the laser light before it can reach the resonant matching point. Depending on the instability!;. overall absorption may be either increased or decreased.

Scattering processes. The most important parametric modes appear to involve coupling of light waves to *electron-plasma waves.* When the scattered wave is light. the mode is known as stimulated Raman scattering.

In Raman scattering the conservation relations require the light to interact with a range of plasma waves whose frequencies are less than or equal to half the light frequency. This means the interaction occurs in the plasma at

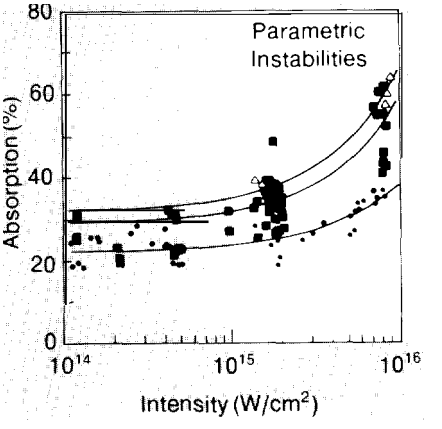

Fig. 11. The dramatic* rise *in absorption above 10^{15} W/cm^2 requires the introduction of other collective absorption mechanisms: parametric instabilities.

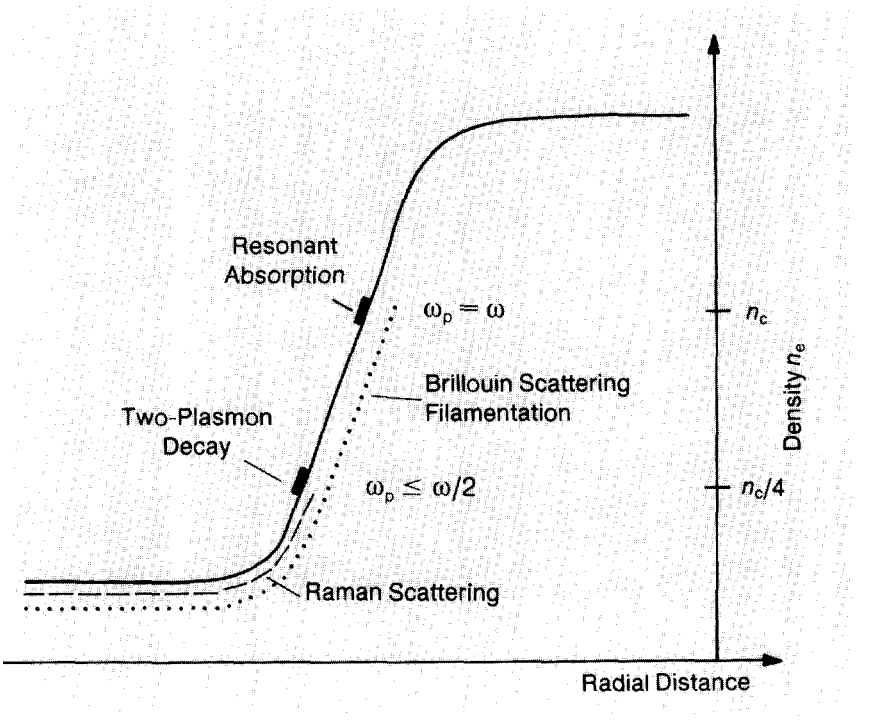

Fig. 12. Resonant absorption occurs in the plasma close to the critical density surface where $w_p = w$. Parametric instabilities couple to plasma waves with frequencies equal to* or less *than w_p, with most occurring in the underdense plasma below w/2. Parametric instabilities include stimulated Raman scattering, two-plasmon decay, stimulated Brillouin scattering, and filamentation instabilities.

densities less than one-fourth n_c where the gradient is not as steep and the interaction region is longer. Thus a broad spectrum of electron-plasma waves are excited that, again through wave breaking, accelerate electrons to high energy. However, in contrast with the short acceleration distances of less than a micrometer for resonant absorption, acceleration distances for Raman scattering can be as long as a millimeter.

.4 process, called *beat wave acceleration,* is being developed that will take advantage of these relatively long acceleration distances to produce extremely energetic particles. Two lasers with a frequency difference equal to the appropriate plasma frequency are used to enhance the plasma-wave amplitude over that generated by Raman scattering itself. The resulting high-velocity and large-amplitude plasma waves may be capable of accelerating particles to the energies envisioned for the next generation of high-energy physics experiments. Although numerous practical problems must be solved, this scheme could produce a relatively compact high-energy accelerator.

When the plasma frequency is *exactly* half the laser frequency, a parametric interaction called two-plasmon decay occurs. In this case, the incident light decays *directly* into two electron-plasma waves, both of frequency o/2, and no light is scattered. Because two-plasmon decay depends even more strongly on the density scaleheight and the temperature of the plasma than does Raman scattering, it is not considered to be a significant absorption mechanism.

The longer interaction regions for Raman scattering imply that the hot-electron temperature should be much higher than that predicted for resonant absorption. Our simulations (Fig. 13) confirm this prediction, with hot-electron temperatures climbing to over 10^3 keV at intensities of 10^{16} W/cm^2. This, of course, is very detrimental for laser fusion.

On the other hand. it should also be noted from Fig. 13 that absorption due to these mechanisms drops to less than 1 per cent of the laser light at 10^{16} W/cm^2. Apparently, the extreme energies of the hot electrons cause a strong damping of the electron-plasma waves, which, in turn, reduces the absorption by these mechanisms. Thus, stimulated Raman scattering must *not* be responsible for the dramatic increase in the observed overall absorption.

There are several mechanisms that. potentially, could explain the increased absorption. The first is Brillouin scattering, which is identical to Raman scattering except the light couples to *ion sound waves* rather than electron-plasma waves. Our calculations indicate. however, that the heating rate from such an ion-based mechanism is significantly lower than for Raman scattering and may be of importance only for the shorter wavelengths.

Extreme intensities also produce self-focusing and filamentation instabilities of the incident light, which, at least in the general sense, are viewed as parametric instabilities. At high intensities, the ponderomotive force of the light literally pushes plasma aside to form channels of less dense plasma but of increased light intensity (Fig. 14). Because the index of refraction is directly related to n_e, such action causes the index to decrease and curves the beam even further into the high-intensity region. Self-focusing refers to the case in which most of the beam is pulled together into a single, intense region; filamentation refers to the case in which intensity peaks are independently reinforced so that the beam breaks into several individual beams. Both of these effects have been observed in numerous experiments at both long and short wavelengths. However, our calculations show that these instabilities build only about as rapidly as Brillouin scattering, and thus they cannot account for the increased absorption.

Theoretically, a number of other parametric instabilities at the critical surface have been identified. Our original simulations, however, showed that the steep density gradients induced by the ponderomotive force severely reduced the instabilities, making them negligible. What then was the mechanism responsible for the dramatic increase in absorption above 10^{15} W/cm^2? Perhaps the key to the puzzle was the behavior of the density gradient for longer times. If, as suggested earlier, the steep gradient dissipated, absorption due to parametric instabilities could become important.

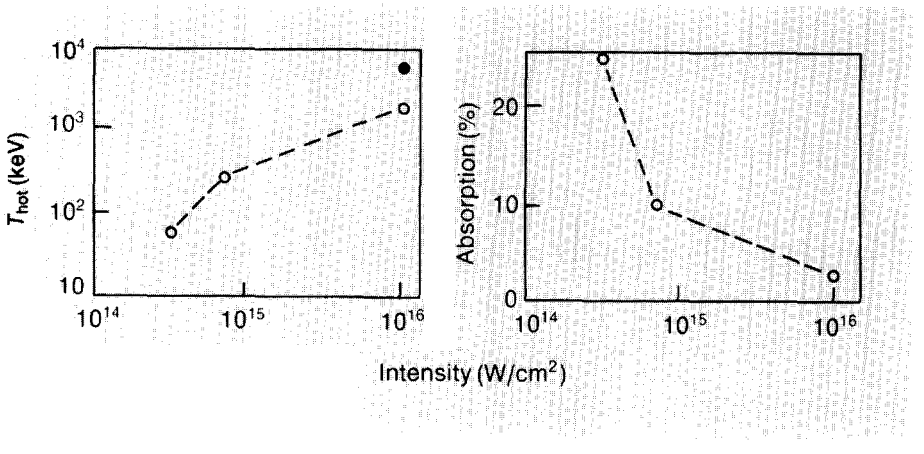

Fig. 13. WAVE simulations showing the effect of Raman scattering on hot-electron temperature absorption, The solid circle in the hot-electron temperature plot is for a somewhat lower density plasma than the open-circle points but all results show very high temperatures at laser intensities of 10^{16} W/cm^2.

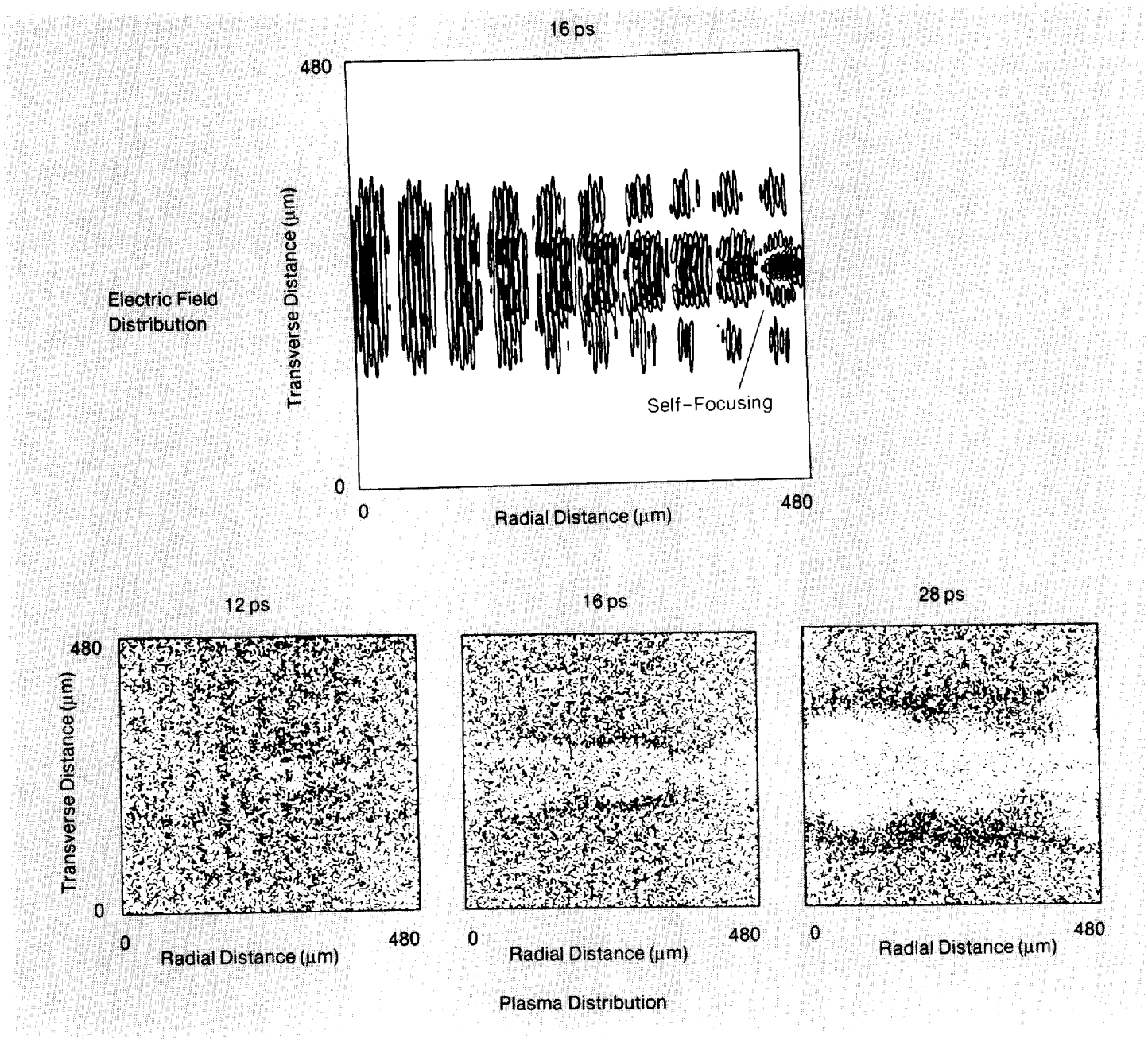

Fig. 14. Self-focusing. All four panels depict a WAVE simulation at the same region in space. The top panel shows electric field lines at 16 picosecond. Although the "laser beam" for this simulation is actually two colinearly propagating beams, the results clearly illustrate self-focusing by the way the inner contours converge as the beam moves toward the right. The lower three panels show the distribution of the electron plasma at 12, 16, and 28 picosecond. Here we see plasma pushed aside as time progresses, resulting in a channel in which the light is focused to higher intensity.

A Mechanism for High Intensities

The recent acquisition of more Cray computers at Los Alamos has made possible simulations that run for tens of picosecond rather than only a few picosecond. Figure [5 shows contour plots of the density surface from such a simulation at 1.5 X 10^{15} W/cm^2. Note that the density gradient, which was originally smooth, has broken up and become rough.

Apparently, a bootstrap effect occurs that starts with a small amount of energy being absorbed through parametric instabilities and deposited in plasma waves. The varied motions of these waves roughens the surface of the steep gradient, the roughness causes the gradient to have less effect on reducing the instabilities, and more energy is absorbed. The result is a substantial increase in absorption from about 25 to 60 per cent. At the same time the hot-electron temperature increases by a factor of 2 or 3 over that calculated for resonant absorption on the initially smooth surface. Also, with a rough surface the angle of acceleration for the hot electrons becomes much broader, and these particles arc shot out in all directions. including inward toward the target.

At 10^{16} W/cm^2 the effect takes place much more rapdily, and the surface becomes even more turbulent. The parametric instabilities at the critical density that were suppressed by the sharp gradient now, at high intensity. appear to become dominant. This process best explains both the increased hot-electron temperatures and the rise in absorption observed at high intensities.

What, then, is our overall picture? We see that the large amplitude of the laser radiation drives the plasma into a highly nonequilibrium state. It is so far from equilibrium that classical shock waves are altered. The region of resonant absorption corresponds essentially to a *phase transition* between hot plasma with laser light and colder plasma without laser light. In this region rarefaction shocks are generated that have very different properties from conventional shock waves. Matter is thus put into an extremely unusual state that is probably only reproduced in exotic astrophysical environments.

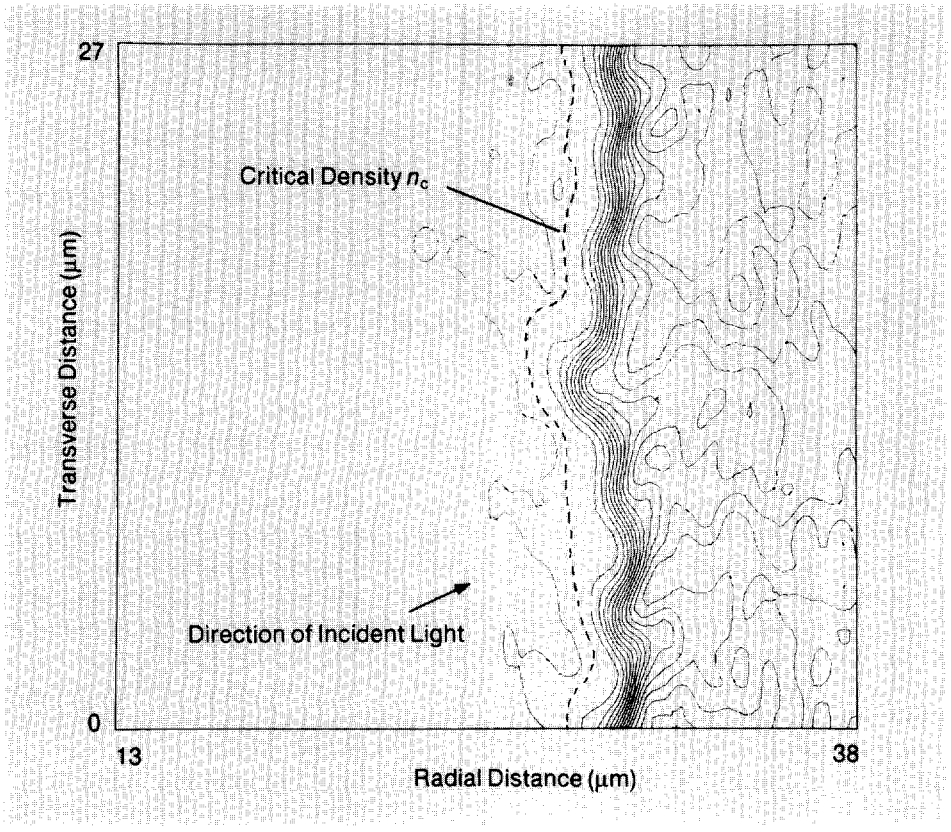

Fig. 15. A WAVE simulation that illustrates with ion-density contours the roughness that builds up on the surface of the density gradient after twenty picosecond, The laser light here has an intensity of 1.5 X 1O^{15} W/cm^2, is incident at an angle of 20 degrees to the surface normal, and is polarized in the plane of the figure. At higher intensities the roughness builds up even more quickly.

Fast-Ion Generation

One of the more exciting features of this unusual state of matter is the generation of *ion jets* (depicted in the opening artwork). As it turns out, these jets are another manifestation of collective effects, because, just as collective effects from the light control the absorption of laser energy, collective effects *in the plasma* dominate the transport of electrons. Specifically, the pressure of hot electrons in the corona can collectively accelerate coronal ions to extremely high energies by collisionless processes.

In the simplest model a small number of hot electrons are stripped from the face of the density gradient and leave the target. These few electrons create an imbalance of charge, and electrostatic potentials of hundreds of kilovolts develop that are unable to bleed off through the target support stalk. Thus, an electrostatic sheath of positive coronal ions is formed that confines the remainder of the electrons. Initially, hot electrons are still projected outward, but they must work against the high potential of the sheath, The net result is a "bounce" in which electrons are redirected inward and positive ions are accelerated outward.

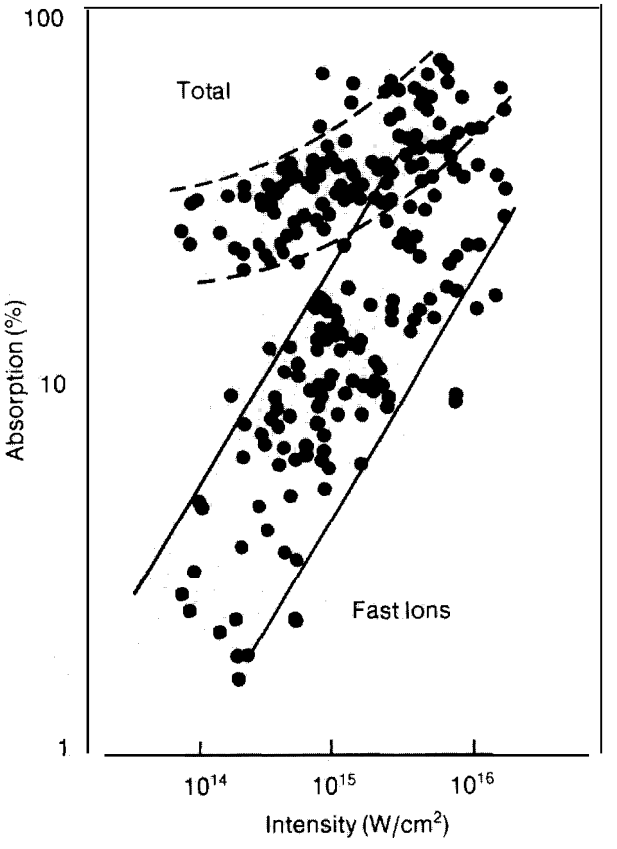

Fig. 16. These data from the Helios laser facility clearly show that at higher intensities a significant fraction of the total absorbed energy appears in the form of fast ions. Targets included spheres that ranged, in diameter, from 200pm to several millimeters and, in material, from plastic to gold. Much of the scatter in the data is due to small-scale fluctuations in intensity across the target and to finite sampling of ions with respect to angular distribution. Within this scattering, there is little difference in fast-ion energy due to changes in the atomic number of the target.

Experimental measurement of the fast-ion energy shows that a substantial fraction of the absorbed laser light goes into fast ions. particularly at high intensity (Fig. 16). Theoretical calculations based on the fraction of energy lost by an electron when it is reflected indicate that, if an electron has only a *single chance* to bounce off the electrostatic sheath. the fraction of energy in fast ions cannot exceed 5 to 10 per cent. Thus we infer that a mechanism exists to trap the electrons in the corona, allowing them to lose more of their energy to fast ions. Known generically as *flux-limited transport,* this mechanism must somehow reduce the mean-energy penetration velocity to less than that for simple diffusion. One potential candidate for this process is the generation of intense magnetic fields by the high-energy electrons themselves.

If illumination of the target is not uniform, as is the case for a finite laser spot, the beam creates a temperature gradient ∇T tangent to the illuminated surface and a strong density gradient of electron plasma ∇n_e normal to the surface. As shown in Fig. 17 (a), these mutually perpendicular gradients generate a magnetic field B, with field lines encircling the spot, at a rate given by

$$\frac{\partial \mathbf{B}}{\partial t} = -\nabla \times \mathbf{E} = (\nabla n_e \times \nabla T)/n_e . \quad (8)$$

Typical values of the parameters in Eq. 8 yield an extraordinarily high value for $\partial \mathbf{B}/\partial t$. For example, with a density gradient of 10 inverse μm, a laser spot size of 100 μm, and a peak temperature in the plasma of 50 keV, a magnetic field equal to a full megagauss can be reached in 1 picosecond. In the time it takes an ejected hot electron to cross the laser spot the field is strong enough to reduce its gyromagnetic radius to less than the density scaleheight. As a result, hot electrons can no longer stream freely from or into the target but are confined by the magnetic field close to the surface.

Furthermore, simulations with our VENUS code show that the electric and magnetic fields can drive the trapped electrons along the target surface at velocities close to the speed of light ($v = cE/B$). This rapid drift (Fig. 17 (b)) reduces the inward transport of electrons under the laser spot and carries some of the electrons and their energy great distances across the target. Moreover, electrons drift along surfaces of constant magnetic field, and a considerable number of them end up circulating around the edge of the spot where the field is strongest.

The result of this pileup of electrons around the spot is a dramatic increase in their effective pressure P that produces a strong electric field, $\mathbf{E} = -\nabla P/n_e$, directed parallel to the density gradient over the spot (Fig. 17 (c)), This field accelerates ions, producing an ion jet, or plume, normal to the target surface.

Figure 18—despite the resemblance, noted by thc Antares experimental team, to a certain extraterrestrial—is an x-ray image of a spherical target at Antares. The target is being hit with six laser beams simultaneously, and five of the impact regions can be seen in the photograph. The resulting distribution of' emitted x rays demonstrates in a vivid manner the existence of the intense magnetic fields that circle the laser spots. Between the "eyes" of the extraterrestrial is a narrow region of significant x-ray emission formed where the magnetic field lines from adjacent spots meet and, because of their opposite polarity, cancel. As a result of the null magnetic field, electrons arc no longer trapped. and energy can be releascd. This effect was first seen dramatically! on spheres, flat targets, and cylindrical targets in experiments at Hclios where, in reference to the Martian features, they were dubbed "canals."

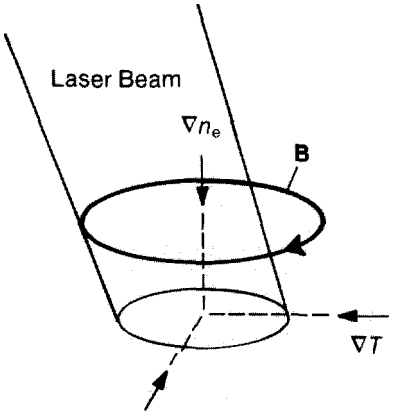

(a)

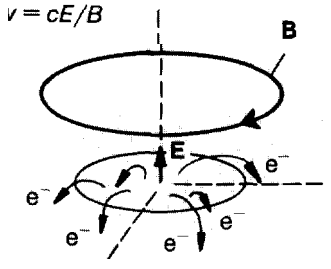

(b)

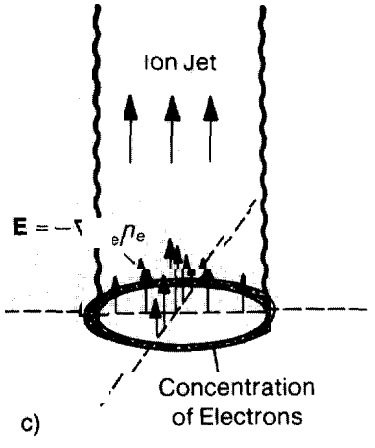

c)

Fig. 18. An ~1-keV x-ray image of the surface of a target being hit simultaneously by the six laser beams of Antares. The narrow region of x-ray emission at the center of the photo is evidence of strong magnetic fields encircling each laser spot; here the fields from adjacent spots cancel, allowing the electrons to move freely into the target rather than being trapped above the surface.

Fig. 17. (a) At the surface of a target, a finite laser beam creates mutually perpendicular density and temperature gradients (∇n_e and ∇T, respectively) that generate an intense magnetic field **B** *encircling the spot. (b) This magnetic field confines hot electrons close to the surface of the target, but they are free to drift sideways under the influence of both magnetic and electric fields with a velocity v given by cE/B. In this manner electrons are driven away from the center of the spot at velocities close to the speed of light with many concentrating at the edge of the spot where the magnetic field is highest. (c) The resulting electron pressure P_e generates high electric fields over the region, and these fields accelerate ions upward, forming the ion jet.*

Ion Jets. To summarize, then, inhomogcneities of tcmpcraturc and density around a laser spot create intense magnetic fields that trap and channel the flow of the hot electrons. The pressure from these trapped electrons generates intense electric fields normal to the surface that accelerate ions, forming a jet. A partial image of one jet has been captured (Fig. 19) with a pinhole camera that separately images x rays emitted from the target and ions accelerated out of the plume. What are the properties of such a jet?

Figure 20 shows the angular distribution of ions leaving a flat disk target that is largc compared to the size of the laser spot. These data were gathered on a *single* laser shot. using three sets of calorimeters filtered to give different energy thresholds for the ions. The plume has a halfwidth at half maximum of about 10 degrees. in excellent agreement with particle simulations using VENUS.

For targets smaller than about a millimeter. including small spheres, the effect is washed out and the ion angular distribution becomes more isotropic. The effect is also washed out in thin targets where electrons can travel from the laser spot by reflexing through the shell and disrupting the current flow that creates the magnetic fields.

The acceleration of' ions in a jet is equivalent to that achieved using intense pulsed-power ion diodes, only here the intensity is much higher than for any conventional diode. In fact, these accelerated ions might be directed at a second target to drive a fusion reaction, except that the collimation of the ion jet is not sufficient.

Experiments also suggest that at high intensity the ion emission may remain high even when the illumination is more uniform. At this point no theory has been devised that conclusively reproduces this effect.

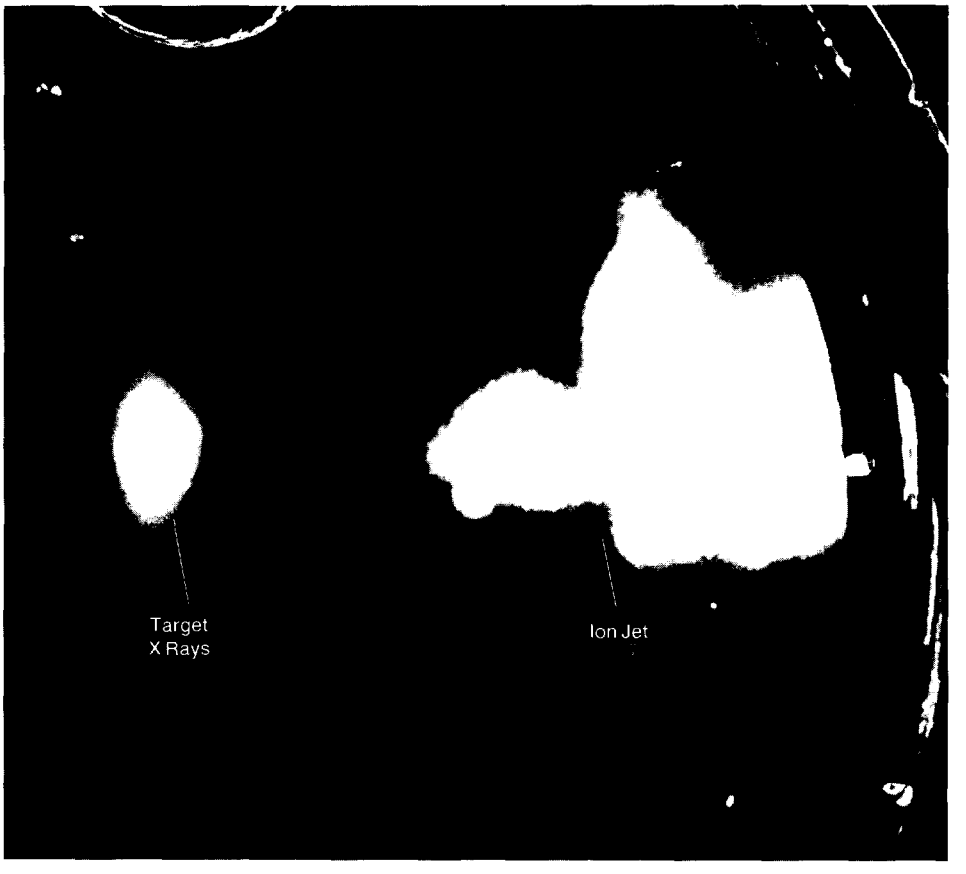

Fig. 19. A sideways image of a portion of an ion jet is captured here by superimposing two negatives: the first is a record of x rays emitted at the surface of the target during one shot, and the second is a record of ions scattered sideways out of the plume during another identical shot. The scattered ions create tracks in a plastic emulsion that is viewed with dark field imaging techniques. The early part of the jet closest to the target is not visible because essentially all the ions are accelerated in the direction of the jet; only after the plume has developed turbulence do a significant number of ions get accelerated sideways toward the emulsion. The later part of the jet is obscured by the round port through which the event was recorded.

Ion Energies. Measurements of the ion velocity distributions with magnetic analyzcr spectrometers indicate that, independent of the target material, much of-the ion energy is carried by hydrocarbons that arc surface contaminants. Such energy partitioning is due, in part, to the favorable acceleration of ions with low atomic number. Although the energy spectrum of' this multispecies ion expansion is remarkably complex-and thus difficult to calculate theoretically-its gross properties arc deceptively simple.

The mean energy of the ions is not far above that required to penetrate a nickel filter with a thickness of 0.5 μm, so we can determine an "ion spectrum" in the form of transmission curves using filtercd calorimeters (Fig. 21). Not only are the resuiting curves well behaved, but the data can

readily be fit to an isothermal expansion model. This model works well using parameters obtained directly from bremsstrahlung measurements if we assume that Z/.4, the ratio of atomic number to atomic mass, is approximately 1/2 (a value more typical of light ions such as carbon than of heavy ions). The transmission data are useful in evaluating target design concepts, for example, in determining what fraction of the ion energy will be absorbed, and thus exploited, by the various masses of a specific target design.

Very heavy ions (such as tantalum and gold) have appreciably shorter stopping range than protons or carbon and are thus more effective in driving the implosion of target material. An analysis of the multispecies ion expansion showed that if low-Z

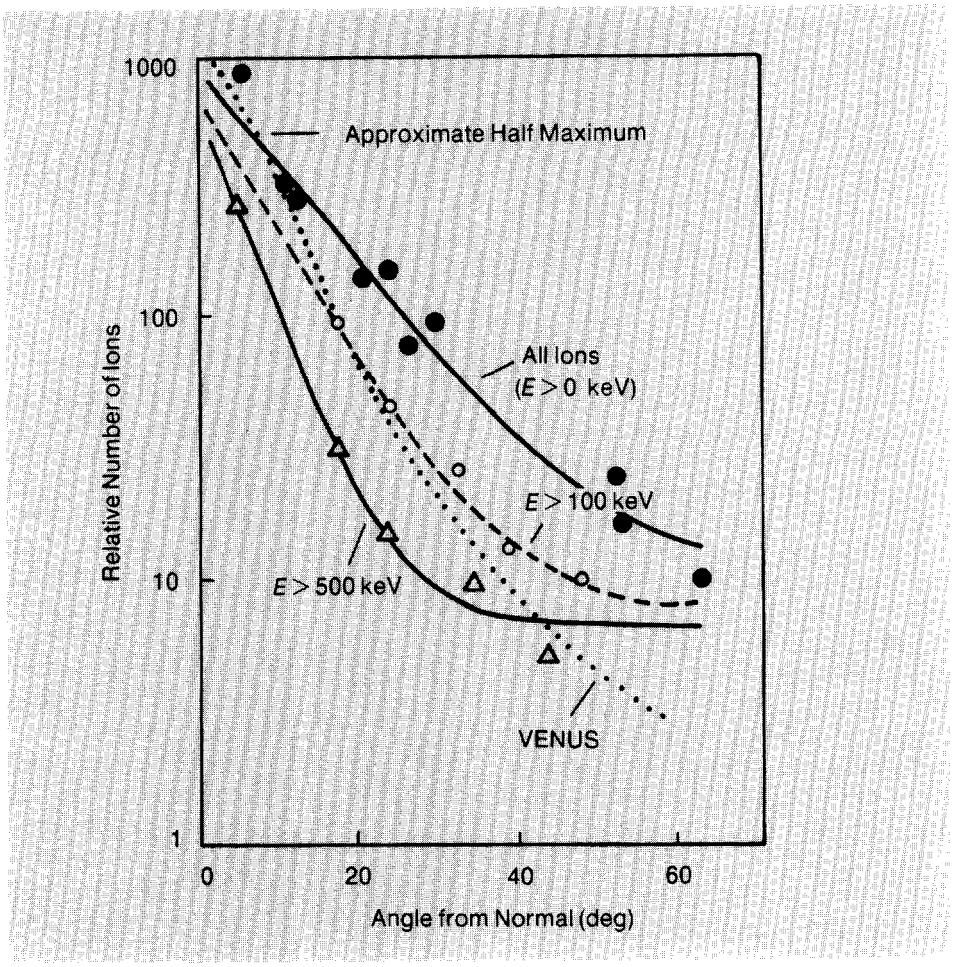

Fig. 20. These data represent the angular distribution of ions in a jet for a single shot at the Helios facility. Three sets of calorimeters were used to measure the relative numbers of ions as a function of angle, each filtered for a different energy threshold in keV per atomic mass unit. The width at half maximum of the angular distribution for all ions is about 10 degrees, and, as the energy E of the ions increases, the angular distribution narrows further. The dotted line is a prediction for the angular distribution of all ions from a VENUS simulation.

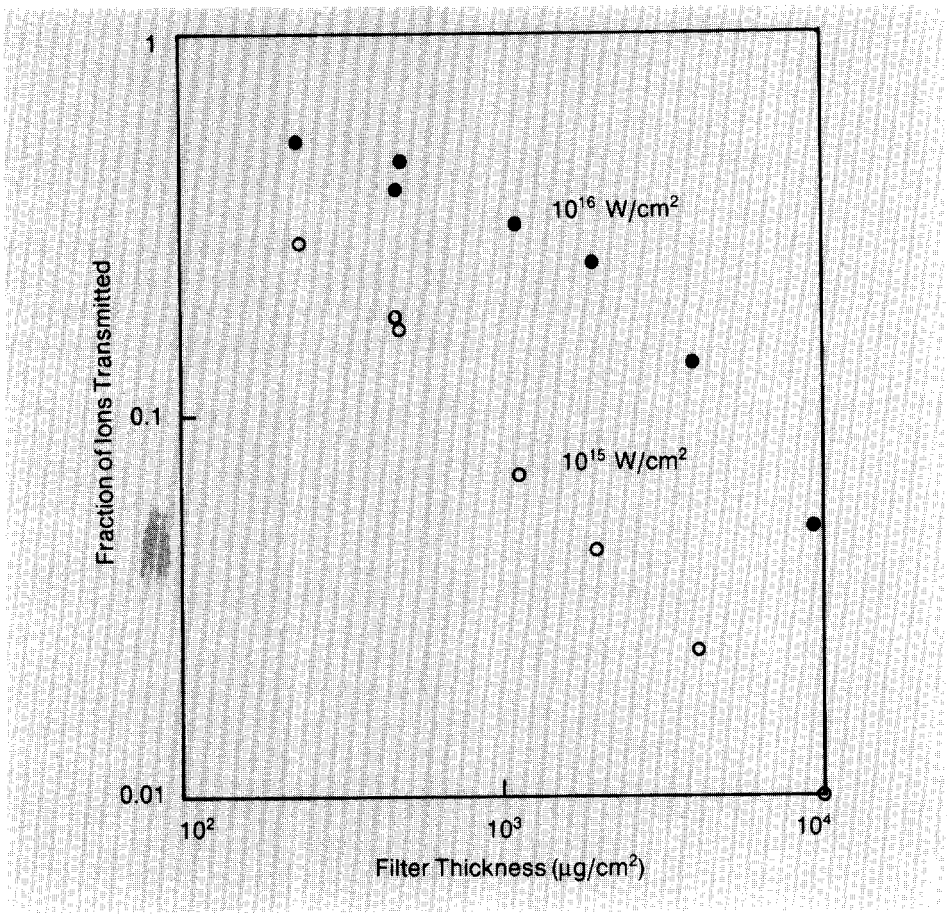

Fig. 21. Ion-range, or transmission, curves for fast ions through nickel filters. The lower intensity shot produced ions of shorter range, that is, lower sound speed, in agreement with a lower temperature in a simple isothermal expansion model.

surface contaminants could be removed, atoms of high-Z target material could be accelerated to similar velocities (the velocity of the fastest proton in a typical expansion is about 2 X 109 cm/s). In an experiment in which hydrocarbons were driven off the surface of tantalum targets by heating to white heat with electron bombardment. we observed energetic tantalum ions, the fastest of which corresponded to an energy of 500 MeV. Spectrometer data confirmed the absence of protons in the expansion and implied that the tantalum ions were as much as 60 times ionized. All this from 10-μm, or 0.1 eV, photons!

Astrophysical and Other Implications

The Antares $C0_2$ laser is able to generate some of the highest energy-density plasmas yet produced in the laboratory. The hot electrons themselves are equivalent to a high-current, Iow-impedance electron-beam source that has a current in excess of 10^8 amperes but voltages only in the hundreds of keV. This results in a source impedance of about a thousandth of an ohm, much lowcr than for any conventional pulsed-power source.

In part because of this low impedance, which prevents very many free electrons from escaping into free space, the intense "thermal" electron beam just described produces our familiar ion jet, which can be described as space-charge-neutralized plasma. traveling at speeds of 10^8 to 10^9 cm/s with collimation maintained over distances of at least 4 meters. In essence. the electron beam is the highest current-density particle accelerator available in any laboratory).

It has been speculated that the extreme high voltages responsible for the acceleration of ions over incredibly short distances could also bc harnessed to produce a *compact,* high-voltage ion accelerator. By using a number of laser beams to strike many targets with appropriate delays between beams, a staged ion accelerator might be built in which the ions from one target are successively accelerated by subsequent targets. This process might be competitive with the beat-wave accelerator described earlier.

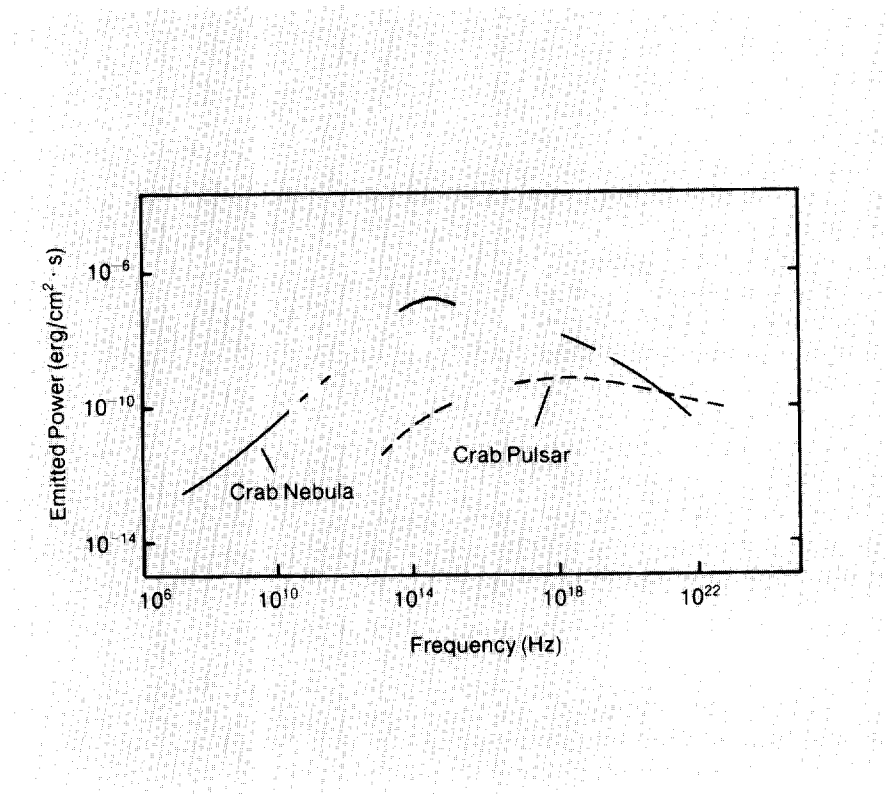

Fig. 22. A comparison of the emitted power as a function of frequency for the Crab Nebula and its pulsar and for $C0_2$ laser targets. The Crab Nebula spectra were adapted from "Galactic Gamma-Ray Sources" by G. F. Bignami and W. Hermsen. **Annual Review of Astronomy and Astrophysics *21(1983):67-108.)***

The ion jets themselves, although perhaps 25 orders of magnitude smaller in time and distance, are reminiscent of the galactic jets that have been so clearly identified from high-resolution radio wave photographs. In fact, an intense emission of microwaves accompanies the laboratory generation of ion jets. There is a striking similarity between the normalized electromagnetic spectrum from a typical Antares target and the equivalent spectrum from the Crab Nebula (Fig. 22). Is this similarity a coincidence or are there common features for both emissions'?

Plasmas created at Helios and Antares were found to be incredibly bright in microwaves: from frequencies of O.1 to 5 gigahertz, over a gigawatt of power was observed; from 26 to 40 gigahertz, 1 to 10 gigawatts were observed. These powers imply that about 0.01 to 0.1 per cent of the incident laser light was converted to microwavcs. The source of the microwaves appears point-like. and the pulse shape, with a rise time of 0.2 nanosecond, nearly follows the laser pulse shape, so the conversion is very rapid. Such surprising emission efficiency may be due to an enhancement in the expanding corona of those plasma waves that couple efficiently to microwave emission.

A mechanism of this type is a strong candidate for explaining microwaves emitted from both galactic jets and from solar flares. Although galactic jets are detected and studied primarily from their radio or microwave emission, a wide variety of processes could generate microwaves in these extended objects. .4 more detailed laboratory investigation of these processes could help us discriminate between the various theories of astrophysical microwave emission.

The ability to *directly* measure in the laboratory not only the emission of electromagnetic radiation but also the *ion motion* of such objects makes study of ion jets particularly attractive and highly complementary to the elegant astrophysical measurements of galactic jets. For example. we can follow the motion of ion jets through other ambient plasmas imposed in the target chamber, learning how energetic ions propagate through ionized plasmas. Does the plume maintain its physical integrity? Is microwave emission altered as the jet strikes another plasma? Theory suggests that the emission in the submillimetcr part of the spectrum will be much higher than at longer wavelengths, a fact that may help explain the match between the spectra for Antares targets and the Crab Nebula.

Also, the intense magnetic fields that help generate ion jets are known to be important for the accretion of matter in white dwarfs. Although we cannot study this process directly, we can study, on a small scale but in great detail, various acceleration mechanisms. then use our results to verify theoretical models. Such verifications would have a profound impact on astrophysical models.

And what of fusion. the initial goal of the Antares research? One very appealing idea (based on a concept that was brought to our attention by Fred Mayer of KMS Fusion. Inc.) combines features of laser and magnetic fusion. Devices that usc magnetic field mirrors have difficulty maintaining stable plasmas for the necessary length of time. Theory for these devices predicts a stable plasma state at high plasma pressures. This state will have particle confinement times substantially greater than those at lower pressures. Unfortunately, conventional particle heating techniques cannot heat the plasma rapidly enough to reach this state without having the confinement destroyed by instabilities at lower pressures.

The extremely rapid heating rate of the CO_2 laser is ideally suited for creating almost instantaneously the high-pressure plasma state predicted to be stable. The direction and energy of the ions can be accurately controlled to produce just the desired conditions. Such a technique would provide both a variety of new options for achieving magnetic fusion energy and interesting combinations of phenomena important to inertial and magnetic fusion.

We have thus discovered a wealth of exotic plasma behavior at high laser intensities. These newfound phenomena allow important experiments to be performed that were not even imagined a decade ago, including bold new approaches to the intricate problem of imitating the thermonuclear burn of stars. ■

Acknowledgments

The authors wish to credit the many dedicated scientists. engineers, and technicians at Los Alamos who have developed the unique laser systems, fabricated the complex targets, developed and debugged the computer codes, devised and built the experimental instruments, and performed the creative and innovative research reflected in this article.

Further Reading

Laser Fusion:

Randolph L. Carlson, James P. Carpenter. Donald E, Casperson, R. B. Gibson, Robert P, Godwin, Richard F. Haglund, John A. Hanlon, Edward L. Jolly, and Thomas F. Stratton. “Helios: A 15 TW Carbon Dioxide Laser Fusion Facility.” *IEEE Journal of Quantum Electronics* 17(1981): 1662.

P. D. Goldstone, G. Allen, H. Jansen, A. Saxman, S. Singer. and M. Thuot. “The Antares Facility for Inertial Fusion Experiments-Status and Plans.” In *Laser Interaction and Related Plasma Phenomena,* Volume 6, pp. 21-32. H. Hera and G. Miley, editors (New York: Plenum Publishing Corporation, 1984).

Thomas H. Johnson. "Inertial Confinement Fusion: Review and Perspective." *Proceedings of the IEEE* 72(1984):548-594.

H. Jansen. "A Review of the Antares Laser Fusion Facility." In Proceedings of IAEA Technical *Committee Meeting in ICF Research. Kobe, Japan, November 14-17, 1983,* Osaka: Institute of Engineering, Osaka University (1984) 284-298.

Plasma Physics:

D. W. Forslund, J. M. Kindel, and E. L. Lindman. "Theory of Stimulated Scattering Processes in Laser-Irradiated Plasmas." *The Physics of Fluids* 18(1975):1002-1016.

D. W. Forslund, J. M. Kindel, and E. L. Lindman. "Plasma Simulation Studies of Stimulated Scattering Processes in Laser-Irradiated Plasmas." *The Physics of Fluids*18(1975):1017-1030.

D. W. Forslund, J. M. Kindel, and K. Lee. "Theory of Hot-Electron Spectra at High Laser Intensity." *Physical Review Letters* 39(1977):284-288.

B. Bezzerides, D. W. Forslund, and E. L. Lindman. "Existence of Rarefaction Shocks in a Laser-Plasma Corona." *The Physics of Fluids* 21(1978):2179-2185.

R. L. Carman, D. W. Forslund, and J. M. Kindel. "Visible Harmonic Emission as a Way of Measuring Profile Steepening." *Physical Review Letters*46(1981):29-32.

W. Priedhorsky, D. Lier, R. Day, and D. Gerke. "Hard X-Ray Measurements of 10.6-pm Laser-Irradiated Targets." *Physical Review Letters* 47(198 1): 1661.

D. W. Forslund and J. U. Brackbill. "Magnetic-Field-Induced Surface Transport on Laser-Irradiated Foils." *Physical Review Letters* 48(1982): 1614-1617.

Fred Begay and David W. Forslund. "Acceleration of Multi-Species Ions in $C0_2$ Laser-Produced Plasmas: Experiments and Theory." *The Physics of Fluids*25(1982):1675.

M. A. Yates, D. B. vanHulsteyn, H. Rutkowski, G. A. Kyrala, and J. Brackbill. "Experimental Evidence for Self-Generated Magnetic Fields and Remote Energy Deposition in Laser-Irradiated Targets." *Physical Review Letters* 49(1982): 1702.

D. R. Bach, D. E. Casperson, D. W. Forslund, S. J. Gitomer, P. D. Goldstone, A. Hauer, J. F. Kephart, J. M. Kindel, R. Kristal, G. A. Kyrala, K. B. Mitchell, D. B. vanHulsteyn, and A. H. Williams. "Intensity-Dependent Absorption in 10.6-µm Laser-Illuminated Spheres." *Physical Review Letters* 50(1983):2082-5.

Allan Hauer, R. Goldman, R. Kristal, M. A. Yates, M. Mueller, F. Begay, D. vanHulsteyn, K. Mitchell, J. Kephart, H. Oona, E. Stover, J. Brackbill, and D. Forslund. "Suprathermal Electron Generation, Transport, and Deposition in $C0_2$ Laser Irradiated Targets." In *Laser Interaction and Related Plasma Phenomena, Volume 6,* p. *479,* H. Hera and G. Miley, editors (New York: Plenum Publishing Corporation, 1984).

D. W. Forslund, J. M. Kindel, W. B. Men, C. Joshi, and J. M. Dawson. "Two-Dimensional Simulations of Single-Frequency and Beat-Wave Laser-Plasma Heating." *Physical Review Letters* 54(1985):558.

Applications:

C. Joshi, W. B. Mori, T. Katsouleas, J. M. Dawson, J. M. Kindel, and D. W. Forslund. "Ultrahigh Gradient Particle Acceleration by Intense Laser-Driven Plasma Density Waves." *Nature* 311(1984):525-9.

F. J. Mayer, H. L. Berk, D. W. Forslund. "A Laser-Initiated Energetic Ion, High Beta Mirror Plasma." To be published in *Comments on Plasma Physics and Controlled Fusion.*

AUTHORS

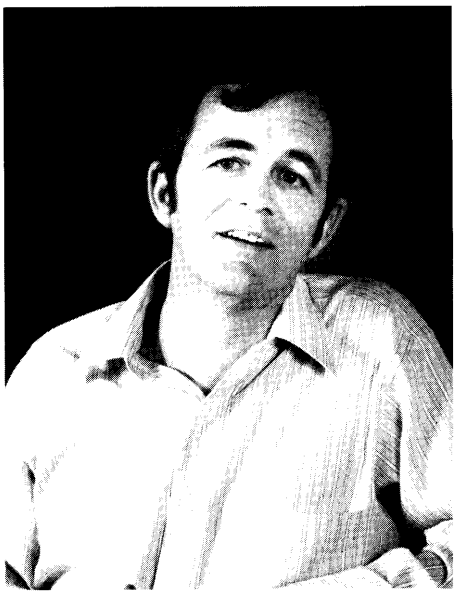

David W. Forslund was born in Ukiah, California, on February 18, 1944. He received his Bachelor of Science from the [University of Santa Clara in 1964 and his Ph.D. in Astrophysical Sciences from Princeton University in 1969. Following two years as a postdoctoral fellow in space physics at Los Alamos, he joined the Magnetic Fusion Theory group and then, in 1972, the Inertial Fusion Theory group with which he has been connected ever since. He served as associate group leader and deputy group leader before being selected as a Laboratory Fellow in 1981. He has made important contributions to space plasma physics. magnetic fusion, high-altitude nuclear effects, and laser plasma interactions as well as numerical simulation techniques for plasmas. A co-recipient of one of the Laboratory's Distinguished Performance Awards in 1982, he is also a member of the American Geophysical Union and the American Astronomical Society and is a Fellow of the American Physical Society. He is active in his local church. serving as a ruling elder, and is Interested in Christian education, serving as president of the board of Covenant Christian School.

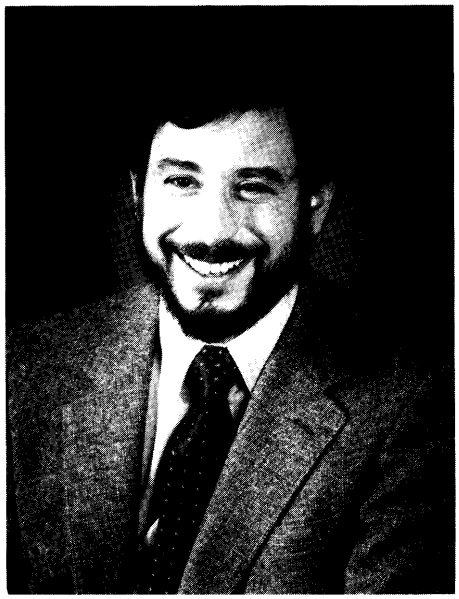

Philip D. Goldstone received his B.S. and M.S. degrees from the Polytechnic Institute of New York in 1971 and 1972, respectively. and his Ph.D. in 1975 from the State University of New York at Stony Brook. One result of his doctoral research was the discovery of a number of new resonances in the sub-barrier fission of actinide nuclei. Joining Los Alamos in 1976 as a postdoc in the Nuclear Physics Group. he studied problems in fission and heavy-ion collisions. In 1977 he joined the fusion effort in the Laser Division and shortly became the Operations Manager of the Gemini CO_2 laser. A year later. excited about the possibilities for laboratory physics research using the incredible power densities available with lasers, he began work on Iaser-driven shock waves. the physics of radiation-driven ICF targets, and the assessment of CO_2 lasers as fusion drivers. Since 1981 he has been Group Leader of the Fusion Experiments and Diagnostics Group in the Physics Division. His current interests include laser acceleration of particles. the physics of highly stripped ions in intense laser fields, and, of course, the dense plasma physics and hydrodynamics of ICF. He has lived in the Jemez Mountains since 1978 with his wife, Joyce, and has been active in the La Cueva volunteer fire department and other community efforts.